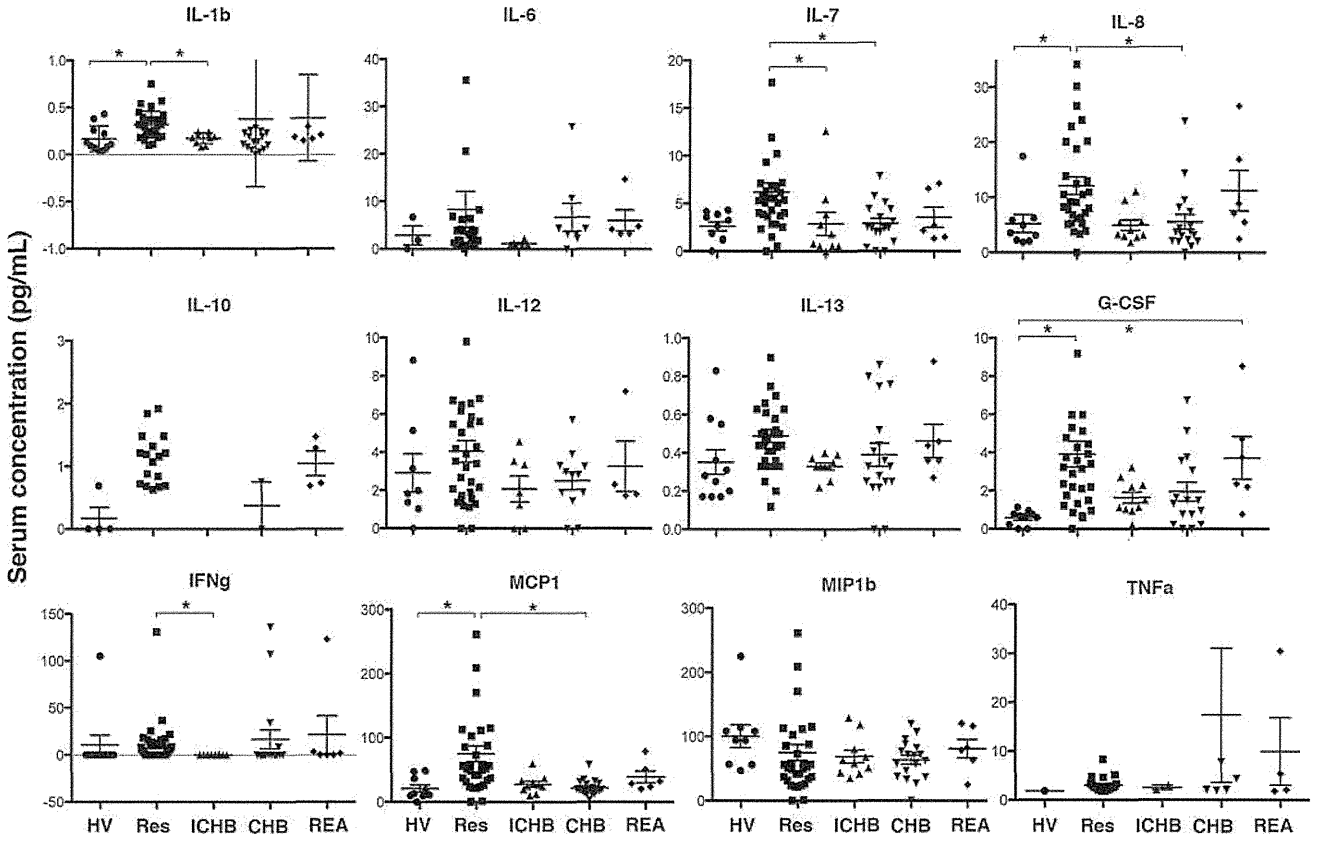

Fig. 1 Serum concentrations of cytokines and chemokines. Serum cytokines and chemokines were measured at the time of diagnosis in HBV reactivation patients and prior to chemotherapy or antiviral therapy in the other groups. The serum concentrations were compared among healthy controls, resolved HBV patients, ICHB patients, CHB patients and HBV reactivation patients. $*P < 0.05$, significant difference between the linked items

the frequencies of HLA-A24 core- and polymerase-specific $CD8^+$ T cells were significantly higher in HBV reactivation patients than in ICHB and CHB patients.

In addition, to evaluate the functional profile of HBV-specific $CD8^+$ T cells we analyzed intracellular IFN-γ production following stimulation with five peptides. Although we did not observe a significant difference in the numbers of IFN-γ producing cells in HBV reactivation patients by HLA-A2 core peptide stimulation, similar results were obtained by tetramer staining following HLA-A24 core and polymerase stimulation (Fig. 2b). We also observed that the number of IFN-γ producing cells in HBV reactivation patients increased by HLA-A2 envelope peptide stimulation (supplementary Fig. 1). These results demonstrated that the frequency of functional HBV-specific $CD8^+$ T cells increased in HBV reactivation patients compared with ICHB and CHB patients.

It was demonstrated that the frequency of circulating $CD4^+CD25^+$ Tregs significantly correlated with the serum viral load in severe CHB patients [16]. To determine whether $CD4^+CD25^+$ and $CD4^+Foxp3^+$ Tregs contribute to liver injury during HBV reactivation, we monitored their numbers in PBMCs. The numbers of $CD4^+CD25^+$ and $CD4^+Foxp3^+$ Tregs had a tendency to be low in HBV reactivation patients compared with the other groups, although the differences were not significant (Fig. 2b, lower panels).

To confirm the inverse correlation between the percentages of HBV-specific $CD8^+$ T cells and the percentages of $CD4^+Foxp3^+$ T cells, we assessed these cells in all patients. As shown in Fig. 2c, a significant inverse correlation was not detected in all patients (white circles), whereas an inverse correlation was noted in HBV reactivation patients (black dots).

PD-1 and CD62L expression on HBV-specific and total $CD8^+$ T cells

The function of antigen-specific $CD8^+$ T cells is impaired, termed "exhaustion," during persistent chronic infection diseases like HBV [17], and exhausted antigen-specific $CD8^+$ T cells express high levels of PD-1 and low levels of CD62L [18]. Based on these findings, we evaluated the expression of PD-1 and CD62L on total $CD8^+$ T cells and

J Gastroenterol (2013) 48:728–737

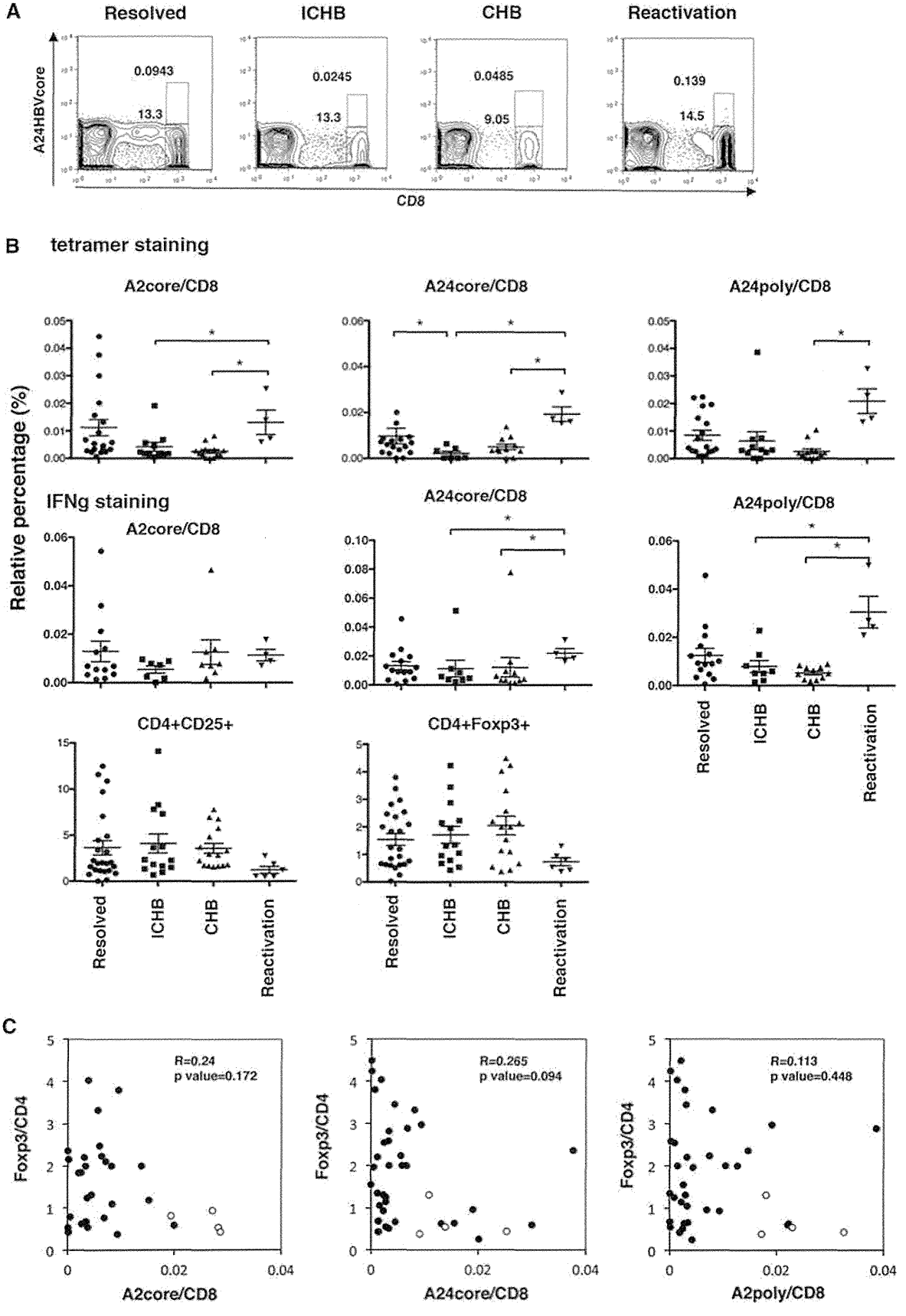

◀ **Fig. 2** **a** FACS analysis using tetramer staining. To detect HBV specific CTLs in the PBMCs, we isolated PBMCs from 4 groups. The samples were stained with PE-conjugated anti-human HLA-A24 HBV core antibody and a PE-Cy5-conjugated anti-human CD8 antibody. **b** Frequencies of HBV-specific $CD8^+$ T cells and $CD4^+$ Tregs. The numbers of HBV-specific $CD8^+$ T cells and Tregs were analyzed by FACS at the time of diagnosis in HBV reactivation patients and prior to chemotherapy or antiviral therapy in the other groups. The *upper panels* show the percentages of HBV-specific $CD8^+$ T cells, among which the *left panel* shows the A2 core, the *center panel* shows the A24 core and the *right panel* shows A24 poly-specific $CD8^+$ T cells. The *middle panels* shows the percentage of IFN-γ producing $CD8^+$ T cells stimulated by peptides for A2 core, A24 core, and A24 poly, respectively. The *lower panels* show the percentages of Tregs, of which the *left panel* shows $CD4^+CD25^+$ Tregs and the *right panel* shows $CD4^+Foxp3^+$ Tregs. $*P < 0.05$, significant difference between the linked items. **c** Relationships between the frequencies of HBV-specific $CD8^+$ T cells and Tregs. The *scatter diagrams* show HBV reactivation patients (*white circle*) and other patients (*black dot*), respectively. The *left panel* shows the negative correlation between $CD4^+Foxp3^+$ Tregs and A2 core-specific $CD8^+$ T cells. The *center panel* shows the negative correlation between $CD4^+Foxp3^+$ Tregs and A24 core-specific $CD8^+$ T cells. The *right panel* shows the negative relationship between $CD4^+Foxp3^+$ Tregs and A24 poly-specific $CD8^+$ T cells

HBV-specific $CD8^+$ T cells to determine whether the $CD8^+$ T cell function in HBV reactivation patients was different from that in the other groups. Although PD-1 expression was higher on circulating HBV-specific $CD8^+$ T cells in ICHB and CHB patients, it was significantly lower on HBV-specific $CD8^+$ cells in HBV reactivation patients (Fig. 3). Curiously, PD-1 expression on HBV-specific $CD8^+$ T cells was low in resolved HBV patients compared with ICHB and CHB patients, indicating that HBV-specific $CD8^+$ T cells in resolved HBV patients may function in a similar manner to those in HBV reactivation patients.

It was also demonstrated that primary CD62L high expressing $CD8^+$ T cells were better at clearing LCMV infection compared with primary CD62L low expressing cells. In addition, CD62L high memory cells underwent robust expansion, and were efficient in preventing chronic LCMV infection [18]. Thus, to address the memory phenotype of cells we examined the expression of CD62L on HBV-specific $CD8^+$ T cells. However, we did not detect any significant differences in the expression of CD62L on $CD8^+$ T cells among the groups although CD62 expression in HBV reactivation patients had a tendency to be lower.

Longitudinal analysis of the frequencies of HBV-specific $CD8^+$ T cells and $CD4^+$ Tregs

To evaluate changes in the frequency of HBV-specific $CD8^+$ T cells during HBV reactivation, we monitored sALT levels, serum HBV DNA levels, percentages of HBV-specific $CD8^+$ T cells and numbers of $CD4^+CD25^+$ and $CD4^+Foxp3^+$ cells in the six HBV reactivation patients. As shown in Fig. 4, when serum HBV DNA was

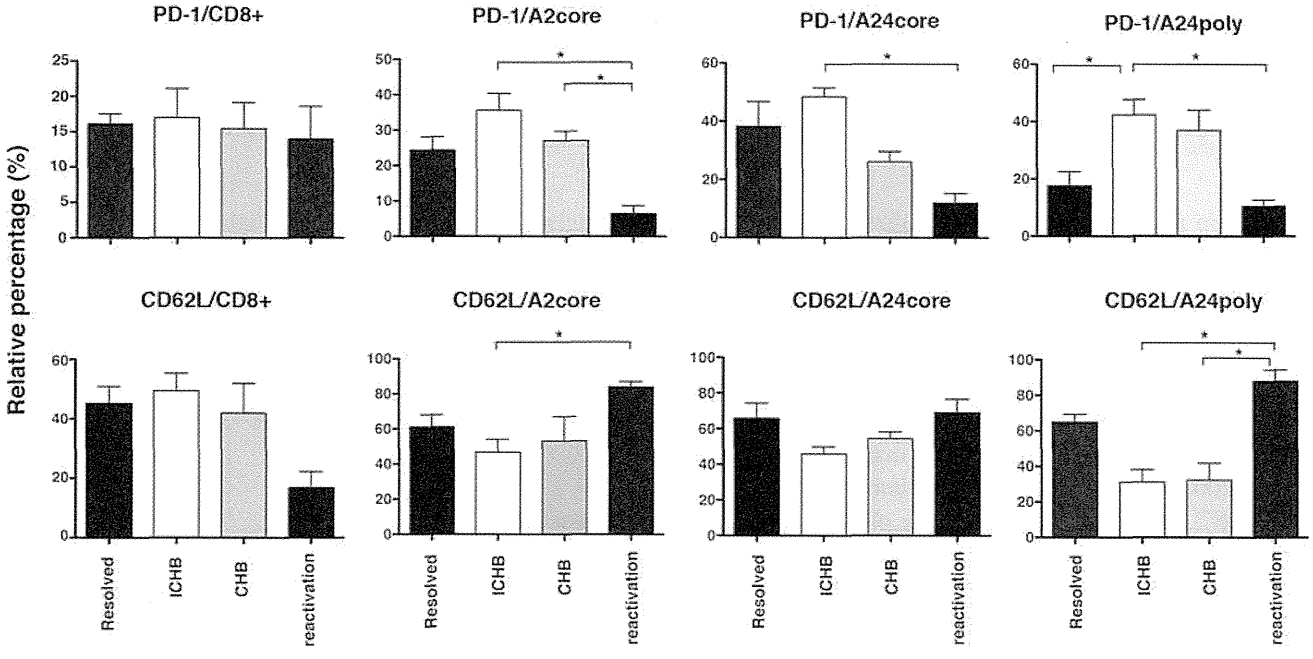

Fig. 3 PD-1 and CD62L expression in HBV-specific and total $CD8^+$ T cells. The PD-1 and CD62L expression levels in HBV-specific and total $CD8^+$ T cells were analyzed by FACS at the time of diagnosis in HBV reactivation patients and prior to chemotherapy or antiviral therapy in the other groups. The *left panel* shows the percentages of PD-1 or CD62L-positive cells in CD8 T^+ cells. The *three right panels* show PD-1 or CD62L-positive cells in HBV-specific $CD8^+$ T cells, respectively. $*P < 0.05$, significant difference between the linked items

J Gastroenterol (2013) 48:728–737

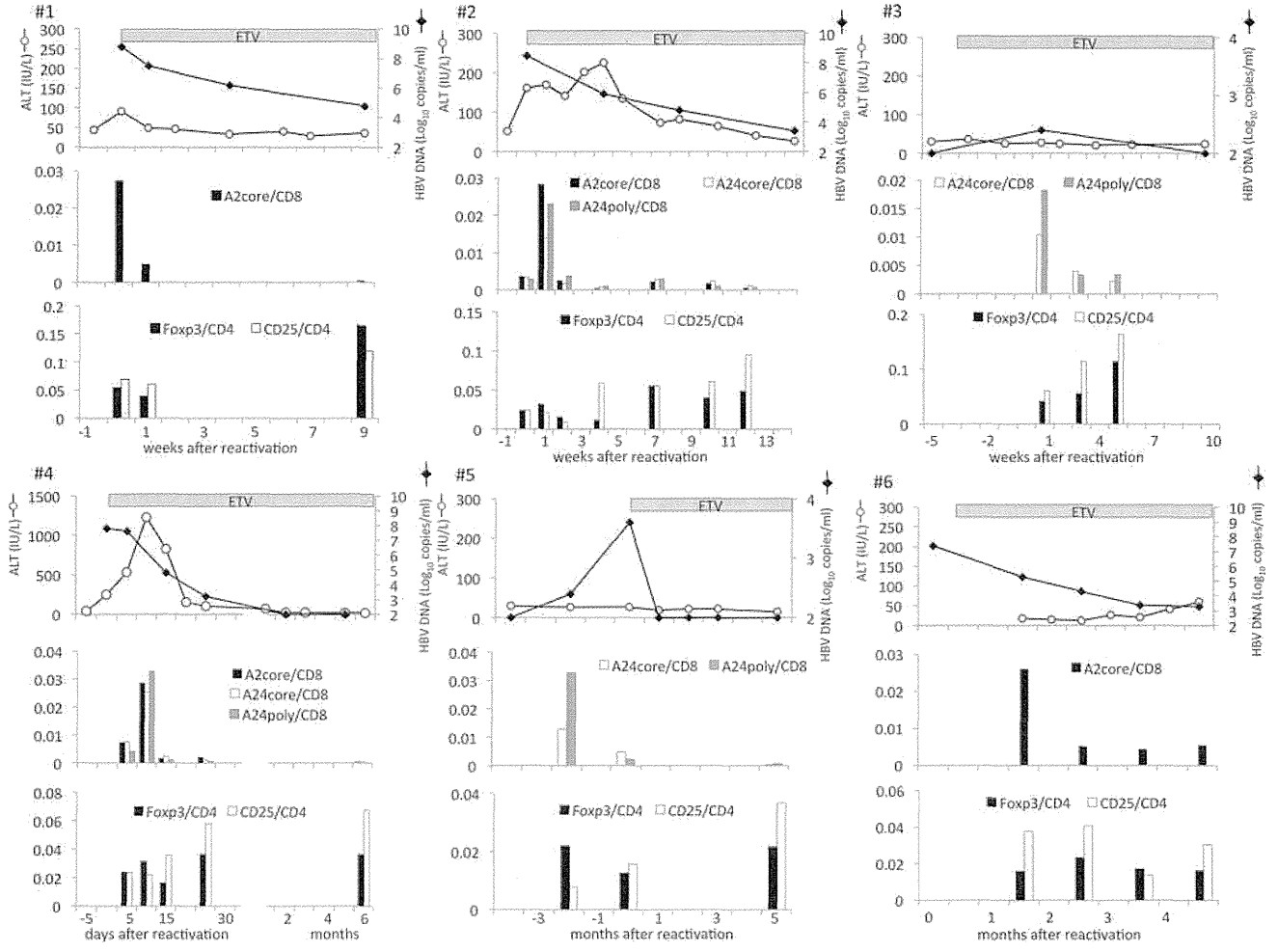

Fig. 4 Longitudinal analysis of the frequencies of HBV-specific $CD8^+$ T cells and Tregs. The *upper panels* show the kinetics of ALT (IU/L) (*white circle*) and HBV DNA (log_{10} copies/ml) (*black diamond*), the *middle panels* show the frequencies of HBV-specific $CD8^+$ T cells and the *lower panels* show the frequencies of Tregs, respectively. All patients were administered entecavir immediately following diagnosis

detected in resolved HBV patients, administration of entecavir was quickly started for all patients to prevent severe hepatitis. HBV-specific $CD8^+$ T cells were detected and reached their peak frequency levels at the onset of HBV reactivation in patients #1 to #6. Interestingly, a high percentage of HBV-specific $CD8^+$ T cells was observed in patient #4 compared with other patients and, consistent with this finding, the sALT level was markedly elevated to about 1200 IU/l, indicating that the number of HBV-specific $CD8^+$ T cells reflected the grade of liver damage, as previously reported [19]. Furthermore, when the numbers of HBV-specific $CD8^+$ T cells were maximal, the numbers of $CD4^+CD25^+$ and $CD4^+Foxp3^+$ T cells were minimal, indicating a negative correlation. Moreover, HBV-specific $CD8^+$ T cells decreased as the sALT level decreased, whereas $CD4^+CD25^+$ and $CD4^+Foxp3^+$ T cells showed tendencies to increase. However, the number of HBV-specific $CD8^+$ T cells in patient #6 did not decrease throughout the time course, although this patient showed tendencies for higher numbers of $CD4^+CD25^+$ and $CD4^+Foxp3^+$ T cells at the time of HBV reactivation. In this patient, the reduction in serum HBV DNA was slow and the sALT levels continued to be elevated. These findings suggest that $CD4^+$ Tregs may suppress an effective immune response against HBV.

Discussion

HBV reactivation is an almost universal event among patients with HBsAg undergoing bone marrow transplantation [20–22]. In retrospective analyses using sensitive serological and virological markers, a high proportion of people with anti-HBc antibodies without HBsAg in their serum also redevelop HBV DNA and HBsAg after bone marrow transplantation [23, 24]. In addition, the prolonged

impairment of immune-mediated control of intrahepatic HBV after extensive immunosuppression leads to reactivation of potential occult infection with HBsAg seroreversion [2]. Thus, although the risk of HBV reactivation during immunosuppression is well known, the mechanism for the induction of HBV reactivation is unclear.

In this study, we demonstrated that six patients with HBV reactivation showed increased numbers of HBV-specific $CD8^+$ T cells, similar to the case for self-limited acute hepatitis B, and that these T cells induced liver damage despite immunosuppression following treatment with an immunosuppressant and anti-cancer drug.

These findings are consistent with a previous report of a strong multifaceted CTL response in patients with acute hepatitis [7]. It is interesting to evaluate the function of antigen-specific $CD8^+$ T cells, including their proliferation and cytokine production, during immunosuppressive drug treatment, because a previous study showed that FK506 did not prevent the generation and proliferation of LCMV-specific T cells, but instead altered their differentiation so that these effector T cells lost their ability to control the virus [25]. Although we analyzed the role of $CD8^+$ T cells under the immunosuppressive status, it seems to be important to analyze macrophages, which produce TNF-α and IL-6 [25].

We found that the ratio of HBV-specific $CD8^+$ T cells was higher in resolved HBV patients than in ICHB and CHB patients, indicating that high viral loads suppress the frequency of these cells [26]. Furthermore, we showed that PD-1 expression on HBV-specific $CD8^+$ T cells was low in resolved HBV patients compared with ICHB and CHB patients, demonstrating that these cells can restore their function. These findings suggested that resolved HBV patients have numerous and functionally recovered HBV-specific $CD8^+$ T cells, and therefore, they may easily develop severe hepatitis once HBV reactivation is induced. This hypothesis was confirmed by a report that acute hepatitis in resolved HBV patients has a higher mortality rate than acute hepatitis in HBV-positive patients [23].

In addition, we found that the frequencies of HBV-specific $CD8^+$ T cells and $CD4^+Foxp3^+$ Tregs were reversible at the onset of HBV reactivation. These observations may imply that the reduction of $CD4^+Foxp3^+$ Tregs triggered the induction of antigen-specific CTLs. Although the effects of $CD4^+Foxp3^+$ Tregs are generally nonspecific or occur in a bystander manner, preferential inhibition of the antigen-specific T cell response has been observed in some cases, including human HBV infection [27]. In support of our results, Xu et al. [16] demonstrated that depletion of $CD4^+CD25^+$ Tregs led to an increase in HBV antigen-stimulated IFN-γ production and cellular proliferation of PBMCs in HBV-infected patients, and that coculture of $CD4^+CD25^+$ Tregs with effector cells significantly suppressed HBsAg-stimulated IFN-γ production and cellular proliferation. At the time of HBV reactivation in patient #6, when the number of $CD4^+Foxp3^+$ Tregs was increased, the reduction in serum HBV DNA was poor and liver damage was continuous. These findings suggest that a reduction in the number of $CD4^+Foxp3^+$ Tregs may induce an effective immune response.

We also observed that serum IL-7, IL-8 and MCP-1 were significantly higher in resolved HBV patients than in ICHB and CHB patients. However, the group of resolved HBV patients was quite miscellaneous and it remains unknown whether the differences among such cytokines and chemokines are responsible for HBV.

It has been demonstrated that IL-7 is required for T cell development and for maintaining and restoring the homeostasis of mature T cells. Administration of recombinant human IL-7 to patients resulted in widespread T cell proliferation, increased T cell numbers, modulation of peripheral T cell subsets and increased T cell receptor repertoire diversity [28]. Furthermore, IL-7 expression by hepatocytes directly controls T cell immune responses to Toll-like receptor signaling in vivo [29]. These observations suggest that IL-7 plays an important role for HBV-specific $CD8^+$ T cell proliferation and that a low level of IL-7 may be involved in the low frequencies of HBV-specific $CD8^+$ T cells in ICHB and CHB patients.

As previously reported, since rituximab therapy is a high risk factor for HBV reactivation, we examined a possible imbalance in serum Th1/Th2 cytokine secretion in HBV reactivation patients. As shown in supplementary Fig. 2, we analyzed the ratio of serum Th1/Th2 cytokines as follows: IFN-γ or IL-12 compared with IL-4 or IL-10. We observed a shift towards IL-10 compared with IFN-γ. However, when we compared IL-12 with IL-4 and IL-10, we observed a shift towards IL-12. Thus, we did not detect an obvious shift towards either Th1 or Th2 cytokines in the serum at the onset of HBV reactivation.

Finally, our study showed that HBV-specific $CD8^+$ T cells are increased at the onset of HBV reactivation despite an immunosuppressive status and declined following resolution of liver disease. In contrast, a reduced number of $CD4^+Foxp3^+$ Tregs was also observed and showed a negative correlation with the frequency of HBV-specific $CD8^+$ T cells. We plan to analyze additional resolved HBV patients prospectively and to clarify the relationships among $CD4^+Foxp3^+$ Tregs, HBV-specific $CD8^+$ T cells and liver damage.

Acknowledgments The authors thank Dr. Yasuhito Tanaka and Shigeru Kusumoto (Nagoya City University School of Medicine) for advice and experimental support. Supported by a grant from the Ministry of Education, Culture, Sports, Science and Technology of Japan and a grant-in-aid for specially promoted research on viral diseases from the Tokyo Metropolitan Government.

Conflict of interest The authors have no conflicts of interest to disclose.

References

1. Hoofnagle JH. Reactivation of hepatitis B. Hepatology. 2009;49:S156–65.
2. Raimondo G, Pollicino T, Cacciola I, Squadrito G. Occult hepatitis B virus infection. J Hepatol. 2007;46:160–70.
3. Yang JD, Roberts LR. Hepatocellular carcinoma: a global view. Nat Rev Gastroenterol Hepatol. 2010;7:448–58.
4. McMahon BJ. The natural history of chronic hepatitis B virus infection. Hepatology. 2009;49:S45–55.
5. Mason AL, Xu L, Guo L, Kuhns M, Perrillo RP. Molecular basis for persistent hepatitis B virus infection in the liver after clearance of serum hepatitis B surface antigen. Hepatology. 1998;27:1736–42.
6. Rehermann B, Ferrari C, Pasquinelli C, Chisari FV. The hepatitis B virus persists for decades after patients' recovery from acute viral hepatitis despite active maintenance of a cytotoxic T-lymphocyte response. Nat Med. 1996;2:1104–8.
7. Chisari FV, Ferrari C. Hepatitis B virus immunopathogenesis. Annu Rev Immunol. 1995;13:29–60.
8. Kimura K, Kakimi K, Wieland S, Guidotti LG, Chisari FV. Activated intrahepatic antigen-presenting cells inhibit hepatitis B virus replication in the liver of transgenic mice. J Immunol. 2002;169:5188–95.
9. Vento S, Cainelli F, Longhi MS. Reactivation of replication of hepatitis B and C viruses after immunosuppressive therapy: an unresolved issue. Lancet Oncol. 2002;3:333–40.
10. Sugauchi F, Tanaka Y, Kusumoto S, Matsuura K, Sugiyama M, Kurbanov F, et al. Virological and clinical characteristics on reactivation of occult hepatitis B in patients with hematological malignancy. J Med Virol. 2011;83:412–8.
11. Barber DL, Wherry EJ, Masopust D, Zhu B, Allison JP, Sharpe AH, et al. Restoring function in exhausted CD8 T cells during chronic viral infection. Nature. 2006;439:682–7.
12. Velu V, Kannanganat S, Ibegbu C, Chennareddi L, Villinger F, Freeman GJ, et al. Elevated expression levels of inhibitory receptor programmed death 1 on simian immunodeficiency virus-specific CD8 T cells during chronic infection but not after vaccination. J Virol. 2007;81:5819–28.
13. Zhang JY, Zhang Z, Wang X, Fu JL, Yao J, Jiao Y, et al. PD-1 up-regulation is correlated with HIV-specific memory CD8+ T-cell exhaustion in typical progressors but not in long-term nonprogressors. Blood. 2007;109:4671–8.
14. Urbani S, Amadei B, Tola D, Massari M, Schivazappa S, Missale G, et al. PD-1 expression in acute hepatitis C virus (HCV) infection is associated with HCV-specific CD8 exhaustion. J Virol. 2006;80:11398–403.
15. Kimura K, Ando K, Tomita E, Ohnishi H, Ishikawa T, Kakumu S, et al. Elevated intracellular IFN-gamma levels in circulating $CD8^+$ lymphocytes in patients with fulminant hepatitis. J Hepatol. 1999;31:579–83.
16. Xu D, Fu J, Jin L, Zhang H, Zhou C, Zou Z, et al. Circulating and liver resident $CD4^+$ $CD25^+$ regulatory T cells actively influence the antiviral immune response and disease progression in patients with hepatitis B. J Immunol. 2006;177:739–47.
17. Blackburn SD, Shin H, Haining WN, Zou T, Workman CJ, Polley A, et al. Coregulation of $CD8^+$ T cell exhaustion by multiple inhibitory receptors during chronic viral infection. Nat Immunol. 2009;10:29–37.
18. Wherry EJ, Ha SJ, Kaech SM, Haining WN, Sarkar S, Kalia V, et al. Molecular signature of $CD8^+$ T cell exhaustion during chronic viral infection. Immunity. 2007;27:670–84.
19. Guidotti LG, Rochford R, Chung J, Shapiro M, Purcell R, Chisari FV. Viral clearance without destruction of infected cells during acute HBV infection. Science. 1999;284:825–9.
20. Au WY, Lie AK, Liang R, Liu CL, Shek TW, Lau GK. Aggressive hepatocellular carcinoma complicating pregnancy after autologous bone marrow transplantation for non-Hodgkin's lymphoma. Bone Marrow Transplant. 2002;29:177–9.
21. Kojima H, Abei M, Takei N, Mukai Y, Hasegawa Y, Iijima T, et al. Fatal reactivation of hepatitis B virus following cytotoxic chemotherapy for acute myelogenous leukemia: fibrosing cholestatic hepatitis. Eur J Haematol. 2002;69:101–4.
22. Seth P, Alrajhi AA, Kagevi I, Chaudhary MA, Colcol E, Sahovic E, et al. Hepatitis B virus reactivation with clinical flare in allogeneic stem cell transplants with chronic graft-versus-host disease. Bone Marrow Transplant. 2002;30:189–94.
23. Kusumoto S, Tanaka Y, Ueda R, Mizokami M. Reactivation of hepatitis B virus following rituximab-plus-steroid combination chemotherapy. J Gastroenterol. 2011;46:9–16.
24. Liang R, Lau GK, Kwong YL. Chemotherapy and bone marrow transplantation for cancer patients who are also chronic hepatitis B carriers: a review of the problem. J Clin Oncol. 1999;17:394–8.
25. Araki K, Gangappa S, Dillehay DL, Rouse BT, Larsen CP, Ahmed R. Pathogenic virus-specific T cells cause disease during treatment with the calcineurin inhibitor FK506: implications for transplantation. J Exp Med. 2010;207:2355–67.
26. Wherry EJ. T cell exhaustion. Nat Immunol. 2011;12:492–9.
27. Alatrakchi N, Koziel M. Regulatory T cells and viral liver disease. J Viral Hepat. 2009;16:223–9.
28. Mackall CL, Fry TJ, Gress RE. Harnessing the biology of IL-7 for therapeutic application. Nat Rev Immunol. 2011;11:330–42.
29. Sawa Y, Arima Y, Ogura H, Kitabayashi C, Jiang JJ, Fukushima T, et al. Hepatic interleukin-7 expression regulates T cell responses. Immunity. 2009;30:447–57.

OPEN ACCESS Freely available online

PLOS | ONE

Immunization with a Recombinant Vaccinia Virus That Encodes Nonstructural Proteins of the Hepatitis C Virus Suppresses Viral Protein Levels in Mouse Liver

Satoshi Sekiguchi[1], Kiminori Kimura[2], Tomoko Chiyo[1], Takahiro Ohtsuki[1], Yoshimi Tobita[1], Yuko Tokunaga[1], Fumihiko Yasui[1], Kyoko Tsukiyama-Kohara[3], Takaji Wakita[4], Toshiyuki Tanaka[5], Masayuki Miyasaka[6], Kyosuke Mizuno[7], Yukiko Hayashi[8], Tsunekazu Hishima[8], Kouji Matsushima[9], Michinori Kohara[1]*

1 Department of Microbiology and Cell Biology, Tokyo Metropolitan Institute of Medical Science, Setagaya-ku, Tokyo, Japan, **2** Division of Hepatology, Tokyo Metropolitan Komagome Hospital, Bunkyo-ku, Tokyo, Japan, **3** Transboundary Animal Diseases Center, Joint Faculty of Veterinary Medicine, Kagoshima University, Korimoto, Kagoshima, Japan, **4** Department of Virology II, National Institute of Infectious Diseases, Shinjuku-ku, Tokyo, Japan, **5** Laboratory of Immunobiology, Department of Pharmacy, School of Pharmacy, Hyogo University of Health Sciences, Chuo-ku, Kobe, Japan, **6** Laboratory of Immunodynamics, Department of Microbiology and Immunology, Osaka University Graduate School of Medicine, Suita, Osaka, Japan, **7** Chemo-Sero-Therapeutic Research Institute, Okubo, Kumamoto, Japan, **8** Department of Pathology, Tokyo Metropolitan Komagome Hospital, Bunkyo-ku, Tokyo, Japan, **9** Department of Molecular Preventive Medicine, School of Medicine, University of Tokyo, Bunkyo-ku, Tokyo, Japan

Abstract

Chronic hepatitis C, which is caused by infection with the hepatitis C virus (HCV), is a global health problem. Using a mouse model of hepatitis C, we examined the therapeutic effects of a recombinant vaccinia virus (rVV) that encodes an HCV protein. We generated immunocompetent mice that each expressed multiple HCV proteins via a Cre/*loxP* switching system and established several distinct attenuated rVV strains. The HCV core protein was expressed consistently in the liver after polyinosinic acid–polycytidylic acid injection, and these mice showed chronic hepatitis C-related pathological findings (hepatocyte abnormalities, accumulation of glycogen, steatosis), liver fibrosis, and hepatocellular carcinoma. Immunization with one rVV strain (rVV-N25), which encoded nonstructural HCV proteins, suppressed serum inflammatory cytokine levels and alleviated the symptoms of pathological chronic hepatitis C within 7 days after injection. Furthermore, HCV protein levels in liver tissue also decreased in a CD4 and CD8 T-cell-dependent manner. Consistent with these results, we showed that rVV-N25 immunization induced a robust CD8 T-cell immune response that was specific to the HCV nonstructural protein 2. We also demonstrated that the onset of chronic hepatitis in CN2-29$^{(+/-)}$/MxCre$^{(+/-)}$ mice was mainly attributable to inflammatory cytokines, (tumor necrosis factor) TNF-α and (interleukin) IL-6. Thus, our generated mice model should be useful for further investigation of the immunological processes associated with persistent expression of HCV proteins because these mice had not developed immune tolerance to the HCV antigen. In addition, we propose that rVV-N25 could be developed as an effective therapeutic vaccine.

Citation: Sekiguchi S, Kimura K, Chiyo T, Ohtsuki T, Tobita Y, et al. (2012) Immunization with a Recombinant Vaccinia Virus That Encodes Nonstructural Proteins of the Hepatitis C Virus Suppresses Viral Protein Levels in Mouse Liver. PLoS ONE 7(12): e51656. doi:10.1371/journal.pone.0051656

Editor: Naglaa H. Shoukry, University of Montreal, Canada

Received March 13, 2012; **Accepted** November 5, 2012; **Published** December 17, 2012

Funding: This study was supported by grants from the Ministry of Education, Culture, Sports, Science, and Technology of Japan; the Program for Promotion of Fundamental Studies in Health Sciences of the Pharmaceuticals and Medical Devices Agency of Japan; and the Ministry of Health, Labor, and Welfare of Japan. The funders had no role in study design, data collection and analysis, decision to publish, or preparation of the manuscript.

Competing Interests: The authors have declared that no competing interests exist.

* E-mail: kohara-mc@igakuken.or.jp

Introduction

Hepatitis C virus (HCV) is a major public health problem; approximately 170 million people are infected with HCV worldwide [1]. HCV causes persistent infections that can lead to chronic liver diseases such as chronic hepatitis, liver cirrhosis, and hepatocellular carcinoma (HCC) [2]. Antiviral drugs are not highly effective in individuals with a chronic infection; furthermore, an effective vaccine against HVC has not been developed. A convenient animal model of HCV infection will greatly facilitate the development of an effective HCV vaccine.

Transgenic mice that express HCV proteins have been generated to study HCV expression [3,4]; however, in each of these cases, the relevant transgenes is expressed during embryonic development; therefore, the transgenic mice become immunotolerant to the transgenic products, and consequently, the adult mice are not useful for investigations of the pathogenesis of chronic hepatitis C. To address this problem, we developed a system that can drive conditional expression of an HCV transgene; our system involves the Cre/*loxP* system and a recombinant adenovirus capable of expressing Cre recombinase [5,6]. Concerns have been expressed that an adenovirus and transient expression of HCV proteins could induce immune responses [5] and, therefore, obscure any evidence of the effect of the host immune responses on chronic liver pathology. Therefore, here, we used a Cre/*loxP* switching system to generate an immunocompetent mouse model

of HCV protein expression; with this system, we could study the host immune responses against HCV proteins.

Folgori et al. (2006) reported effective vaccination of chimpanzees with an adenoviral vector and plasmid DNA encoding the HCV nonstructural region. This technique protected the liver tissues from acute hepatitis, which results when whole animals are challenged with virus [7]. However, this vaccine has not yet been shown to be effective against chronic HCV infection.

Here, we aimed to address how HCV expression causes chronic liver diseases and to provide new options for HCV vaccine development. Using LC16m8, a highly attenuated strain of vaccinia virus (VV), we generated three recombinant vaccinia viruses (rVVs) that each encoded one of three different HCV proteins and found that one recombinant virus (rVV-N25), which encoded nonstructural HCV proteins, resolved pathological chronic hepatitis C symptoms in the liver. We also found that immunization with rVV-N25 suppressed HCV core protein levels in the livers of transgenic mice; moreover, this suppression was mediated by CD4 and CD8 T cells, as has been previously reported [8].

Results

Generation of a Model of Persistent HCV Protein Expression

To produce adult mice that express an HCV transgene, we bred CN2-29 transgenic mice, which carry an HCV transgene, [5,6,9] with Mx1-Cre transgenic mice [10], which express Cre recombinase in response to interferon (IFN)-α or a chemical inducer of IFN-α, poly(I:C) (Figure 1A). Following poly(I:C) injection, the HCV transgene was rearranged, and HCV sequences were expressed in the livers of F1 progeny (CN2-29$^{(+/-)}$/MxCre$^{(+/-)}$ mice) within 7 days after poly(I:C) injection (Figure 1B).

To evaluate the characteristic features of these CN2-29$^{(+/-)}$/MxCre$^{(+/-)}$ mice, we analyzed serum alanine aminotransferase (ALT) and liver HCV core protein levels after poly(I:C) injection. As illustrated in Figure 1C, serum ALT levels increased and reached a peak at 24 h after the first poly(I:C) injection; this elevation appeared to be a direct result of the poly(I:C) treatment, which causes liver injury [11]. After this peak, serum ALT levels dropped continuously until day 4, and then ALT levels began to increase, as did HCV core protein levels. Thereafter, the HCV core protein was expressed consistently for at least 600 days.

Histological analysis showed HCV core protein expression in most hepatocytes of the transgenic mice; these mice showed evidence of lymphocytic infiltration that was caused by the HCV core proteins (Figure 1D and E). These observations, in addition to the modified histology activity index (HAI) scores, indicated that expression of HCV proteins caused chronic hepatitis in the CN2-29$^{(+/-)}$/MxCre$^{(+/-)}$ mice because a weak, though persistent, immune response followed an initial bout of acute hepatitis (Figure S1). Moreover, we observed a number of other pathological changes in these mice – including swelling of hepatocytes, abnormal architecture of liver-cell cords, abnormal accumulation of glycogen, steatosis, fibrosis, and HCC (Figures 1E and F, Table S1). Steatosis was mild in the younger mice (day 21) and became increasingly severe over time (days 120 and 180; Figure S2). Importantly, none of the pathological changes were observed in the CN2-29$^{(+/-)}$/MxCre$^{(-/-)}$ mice after poly(I:C) injection (Figure 1F).

Recombinant Vaccinia Virus Immunization in HCV Transgenic Mice

To determine whether activation of the host immune response caused the reduction with HCV protein levels in the livers of CN2-29$^{(+/-)}$/MxCre$^{(+/-)}$ mice, we used a highly attenuated VV strain, LC16m8, to generate three rVVs [12]. Each rVV encoded a different HCV protein; rVV-CN2 encoded mainly structural proteins, rVV-N25 encoded nonstructural proteins, and rVV-CN5 encoded the entire HCV protein region (Figure 2A). Because rVVs can express a variety of proteins and induce strong and long-term immunity, they have been evaluated as potential prophylactic vaccines [13].

We used western blots to confirm that each HCV protein was expressed in cell lines. Each of seven proteins – the core, E1, E2, NS3-4A, NS4B, NS5A, and NS5B – was recognized and labeled by a separate cognate antibody directed (Figure S3). To induce effective immune responses against HCV proteins in transgenic mice, we injected an rVV-HCV (rVV-CN2, rVV-CN5, or rVV-N25) or LC16m8 (as the control) intradermally into CN2-29$^{(+/-)}$/MxCre$^{(+/-)}$ mice 90 days after poly(I:C) injection (Figure 2B). Analysis of liver sections 7 days after immunization with rVV-N25 revealed dramatic improvement in a variety of pathological findings associated with chronic hepatitis – including piecemeal necrosis, hepatocyte swelling, abnormal architecture of liver-cell cords, abnormal accumulation of glycogen, and steatosis (Figures 2C–E). Collectively, these results demonstrated that only the rVV-N25 treatment resulted in histological changes indicative of improvement in the chronic hepatitis suffered by the transgenic mice.

To determine whether rVV-N25 treatment induced the same effect in other strains of HCV transgenic mice, we analyzed RzCN5-15$^{(+/-)}$/MxCre$^{(+/-)}$ mice, which express all HCV proteins; in these mice, chronic hepatitis was resolved within 28 days of immunization with rVV-N25. Taken together, these findings indicated that rVV-N25 had a dramatic therapeutic effect on both types of HCV transgenic mice (Figure S4).

Treatment with rVV-N25 Reduced the HCV Core Protein Levels in the Livers

To assess in detail the effects of rVV-HCV immunization on HCV protein clearance from the livers of CN2-29$^{(+/-)}$/MxCre$^{(+/-)}$ mice, we monitored the levels of HCV core protein in liver samples via ELISA. We found that within 28 days after immunization the HCV core protein levels were significantly lower in livers of rVV-N25-treated mice than in those of control mice (Figure 3A). Immunohistochemical analysis indicated that, within 28 days after immunization, levels of HCV core protein were substantially lower in the livers of CN2-29$^{(+/-)}$/MxCre$^{(+/-)}$ mice than in those of control mice (Figure 3B). Importantly, neither resolution of chronic hepatitis nor reduction in the HCV protein levels was observed in the mice treated with LC16m8, rVV-CN2, or rVV-CN5. These results indicated that HCV nonstructural proteins might be important for effects of therapeutic vaccines. In contrast, rVV-CN5 which encoded HCV structural and non-structural proteins did not show any significant effects. These results indicated that HCV structural proteins might have inhibited the therapeutic effects of the non-structural proteins. Therefore, it may be important to exclude the HCV structural proteins (aa 1–541) as antigenic proteins when developing therapeutic vaccines against chronic hepatitis C.

In addition, we measured serum ALT levels in CN2-29$^{(+/-)}$/MxCre$^{(+/-)}$ mice from all four treatment groups 28 days after rVV-HCV immunization. Serum ALT levels were not significant-

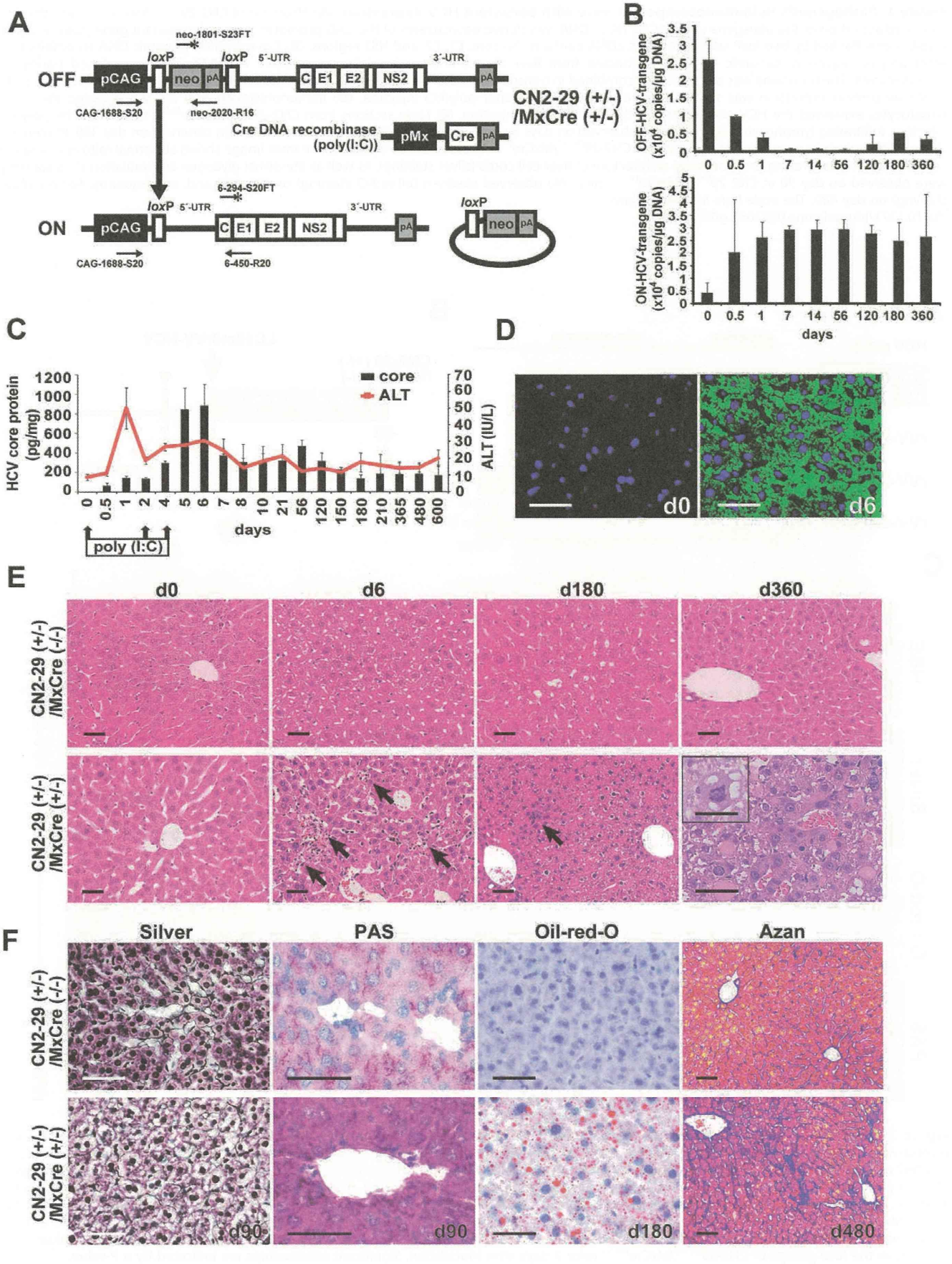
A
neo-1801-S23FT
loxP
loxP
5´-UTR
3´-UTR
OFF
pCAG
neo
pA
C
E1
E2
NS2
pA
CAG-1688-S20
neo-2020-R16
CN2-29 (+/-)
/MxCre (+/-)
Cre DNA recombinase
(poly(I:C))
pMx
Cre
pA
6-294-S20FT
loxP
5´-UTR
3´-UTR
ON
pCAG
C
E1
E2
NS2
pA
loxP
neo
pA
CAG-1688-S20
6-450-R20
B
OFF-HCV-transgene
(x10⁴ copies/μg DNA)
3.5
3
2.5
2
1.5
1
0.5
0
0
0.5
1
7
14
56
120
180
360
ON-HCV-transgene
(x10⁴ copies/μg DNA)
5
4.5
4
3.5
3
2.5
2
1.5
1
0.5
0
0
0.5
1
7
14
56
120
180
360
days
C
HCV core protein
(pg/mg)
1200
1000
800
600
400
200
0
core
ALT
70
60
50
40
30
20
10
0
ALT (IU/L)
0
0.5
1
2
4
5
6
7
8
10
21
56
120
150
180
210
365
480
600
days
poly (I:C)
D
d0
d6
E
d0
d6
d180
d360
CN2-29 (+/-)
/MxCre (-/-)
CN2-29 (+/-)
/MxCre (+/-)
F
Silver
PAS
Oil-red-O
Azan
CN2-29 (+/-)
/MxCre (-/-)
CN2-29 (+/-)
/MxCre (+/-)
d90
d90
d180
d480

Figure 1. Pathogenesis in immunocompetent mice with persistent HCV expression. (**A**) Structure of CN2-29$^{(+/-)}$/MxCre$^{(+/-)}$ and the Cre-mediated activation of the transgene unit. R6CN2 HCV cDNA was cloned downstream of the CAG promoter, neomycin-resistant gene (*neo*), and poly A (pA) signal flanked by two *loxP* sequences. This cDNA contains the core, E1, E2, and NS2 regions. (**B**) Cre-mediated genomic DNA recombination. After poly(I:C) injection, genomic DNA was extracted from liver tissues and analyzed by quantitative RTD-PCR for Cre-mediated transgenic recombination. The transgene was almost fully recombined in transgenic mouse livers 7 days after the injection. In all cases, n = 3 mice per group. (**C**) HCV core protein expression was sustained for at least 600 days after poly(I:C) injection. (**D**) Immunohistochemical analysis revealed that most hepatocytes expressed the HCV core protein within 6 days after injection. (**E**) Liver sections from CN2-29$^{(+/-)}$/MxCre$^{(+/-)}$ mice after the poly(I:C) injection. Infiltrating lymphocytes (arrows) were observed on days 6 and 180; Hepatocellular carcinoma (HCC) was observed on day 360. In contrast, these pathological changes were not observed in CN2-29$^{(+/-)}$/MxCre$^{(-/-)}$ mice after the injection. The inset image shows abnormal mitosis in a tumor cell. (**F**) Hepatocyte swelling and abnormal architecture of liver-cell cords (silver staining), as well as abnormal glycogen accumulation (PAS staining) were observed on day 90 in CN2-29$^{(+/-)}$/MxCre$^{(+/-)}$ mice. We observed steatosis (oil-red-O staining) on day 180 and, subsequently, fibrosis (Azan staining) on day 480. The scale bars indicate 50 μm.
doi:10.1371/journal.pone.0051656.g001

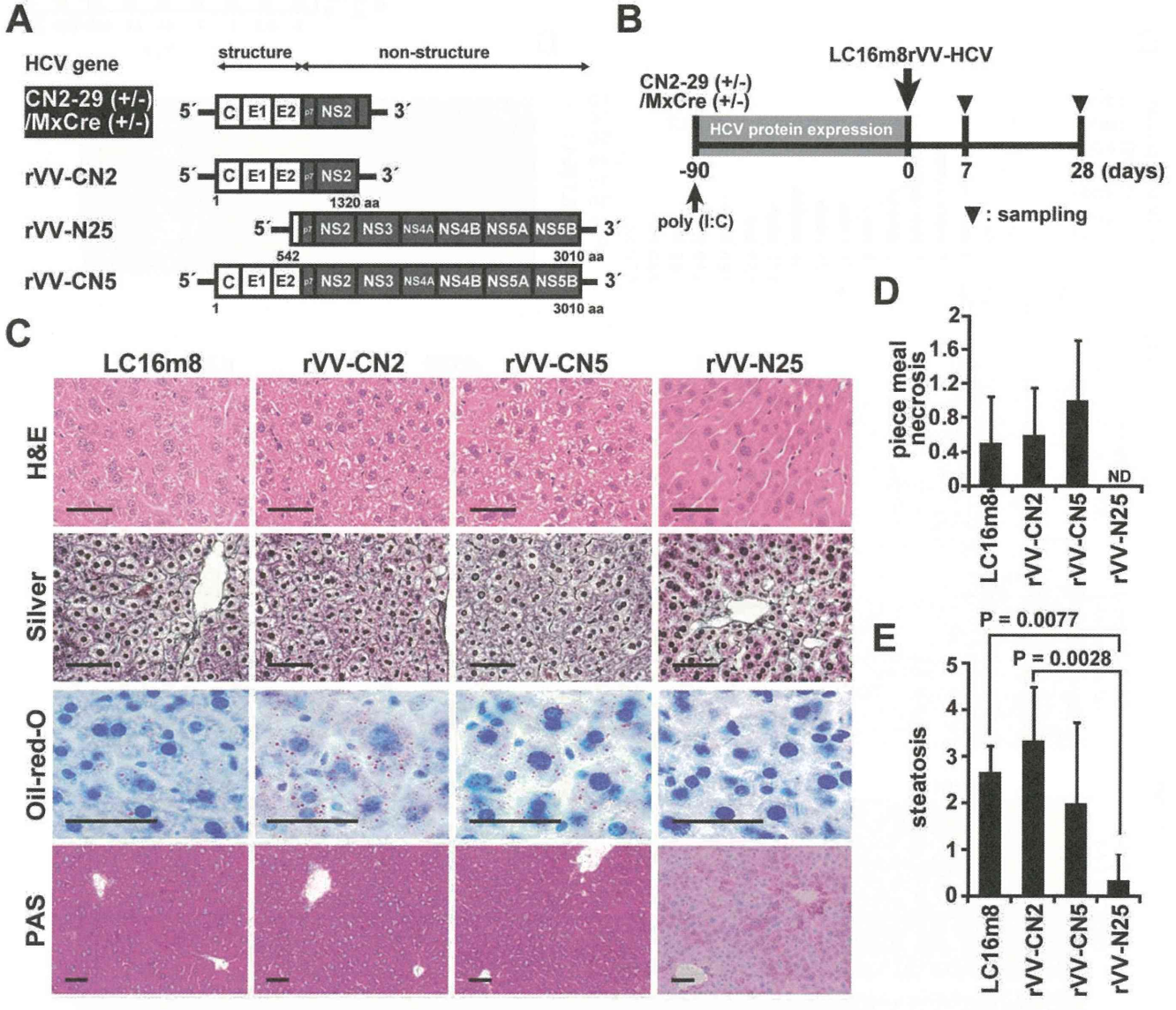

Figure 2. Effects of rVV-HCV treatment on the CN2-29$^{(+/-)}$/MxCre$^{(+/-)}$ mice. (**A**) HCV gene structure in the CN2-29$^{(+/-)}$/MxCre$^{(+/-)}$ mice and recombinant vaccinia viruses (rVV-HCV). MxCre/CN2-29 cDNA contains the core, E1, E2, and NS2 regions. The rVV-CN2 cDNA contains the core, E1, E2, and NS2 regions. The rVV-N25 cDNA contains the NS2, NS3, NS4A, NS4B, NS5A, and NS5B regions. The rVV-CN5 cDNA contains the entire HCV region. (**B**) Four groups of CN2-29$^{(+/-)}$/MxCre$^{(+/-)}$ mice were inoculated intradermally with rVV-CN2, rVV-N25, rVV-CN5, or LC16m8 90 days after the poly(I:C) injection. Blood, liver, and spleen tissue samples were collected 7 and 28 days after the inoculation. (**C**) Liver sections from the four groups of CN2-29$^{(+/-)}$/MxCre$^{(+/-)}$ mice 7 days after the inoculation. The sections were stained with H&E, silver, oil-red-O, or PAS. The scale bars indicate 50 μm. (**D**) Histological evaluation of piecemeal necrosis in the four groups of CN2-29$^{(+/-)}$/MxCre$^{(+/-)}$ mice 7 days after inoculation. (**E**) Histological evaluation of steatosis in the four groups of CN2-29$^{(+/-)}$/MxCre$^{(+/-)}$ mice 7 days after inoculation. Significant relationships are indicated by a P-value.
doi:10.1371/journal.pone.0051656.g002

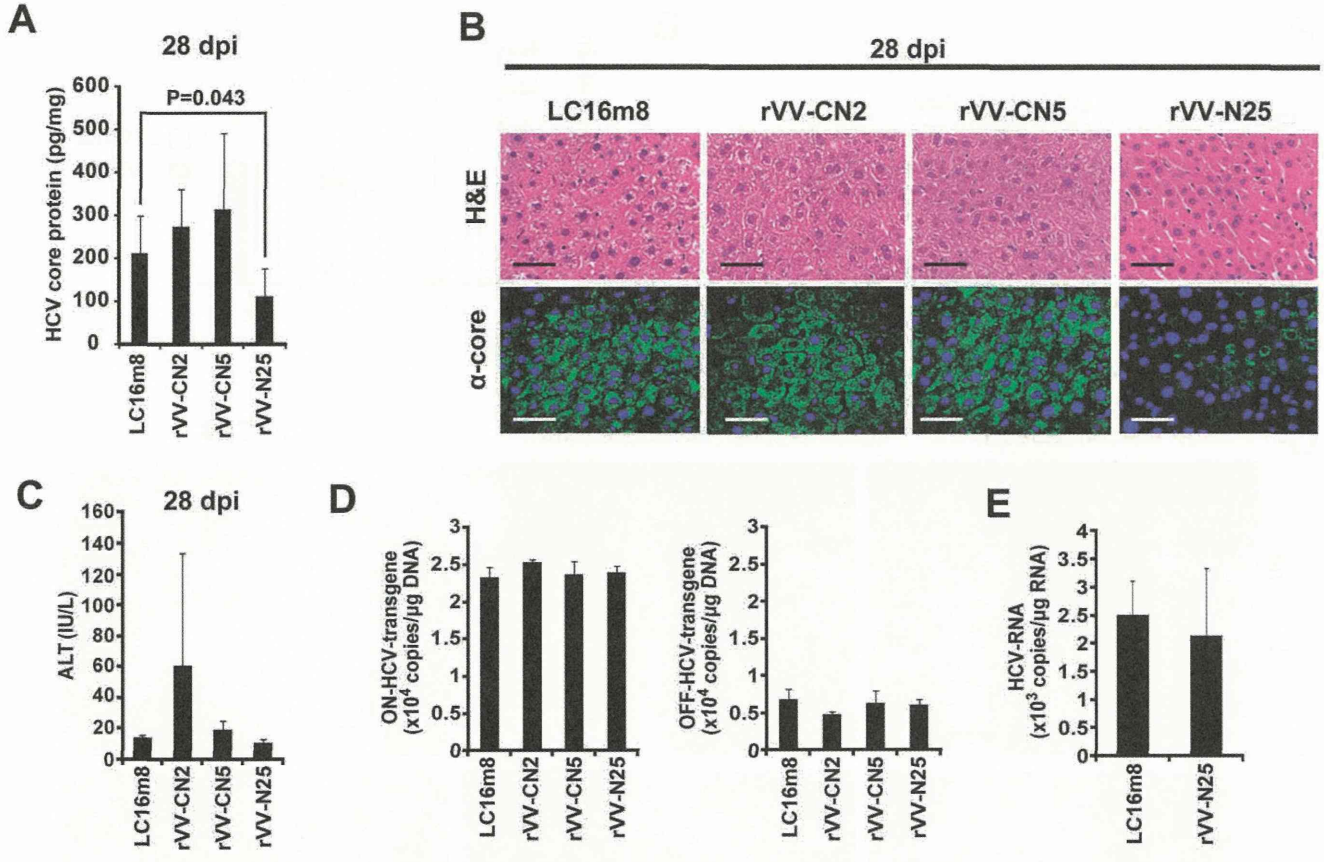

Figure 3. Effects of HCV core protein expression on the livers of CN2-29$^{(+/-)}$/MxCre$^{(+/-)}$ mice inoculated with rVV-HCV. (**A**) Expression of the HCV core protein in the four treatment groups of CN2-29$^{(+/-)}$/MxCre$^{(+/-)}$ mice 28 days after the inoculation. Significant relationships are indicated by a P-value. (**B**) H&E staining and immunohistochemical analysis for HCV core protein in the LC16m8-, rVV-CN2-, rVV-CN5-, or rVV-N25-treated CN2-29$^{(+/-)}$/MxCre$^{(+/-)}$ mice 28 days after the inoculation. Liver sections were stained with the anti-core monoclonal antibody. The scale bars indicate 50 μm. (**C**) Effects of HCV core protein expression on serum ALT levels in the four treatment groups of CN2-29$^{(+/-)}$/MxCre$^{(+/-)}$ mice 28 days after immunization. (**D**) Cre-mediated genomic DNA recombination in the four treatment groups 28 days after immunization. (**E**) Expression of HCV mRNA in the LC16m8- or rVV-N25-treated CN2-29$^{(+/-)}$/MxCre$^{(+/-)}$ mice 28 days after immunization. In all cases, n = 6 mice per group.
doi:10.1371/journal.pone.0051656.g003

ly different in the rVV-N25-treated mice and control mice (Figure 3C); this finding indicated that rVV-N25 treatment did not cause liver injury and that the antiviral effect was independent of hepatocyte destruction.

We hypothesized that the reduction in the levels of HCV core protein in rVV-HCV-treated mice was not caused by cytolytic elimination of hepatocytes that expressed HCV proteins. To investigate this hypothesis, we conducted an RTD-PCR analysis of genomic DNA from liver samples of CN2-29$^{(+/-)}$/MxCre$^{(+/-)}$ mice. The recombined transgene was similar in rVV-N25-treated and control mice 28 days after immunization (Figure 3D). We also measured the expression of HCV mRNA in LC16m8-treated CN2-29$^{(+/-)}$/MxCre$^{(+/-)}$ mice with that in rVV-N25-treated CN2-29$^{(+/-)}$/MxCre$^{(+/-)}$ mice 28 days after immunization; the HCV mRNA levels did not differ between rVV-N25-treated CN2-29$^{(+/-)}$/MxCre$^{(+/-)}$ and control mice (Figure 3E). These results indicated that rVV-N25-induced suppression of HCV core protein expression could be controlled at a posttranscriptional level.

Role of CD4 and CD8 T cells in rVV-N25-treated Mice

Viral clearance is usually associated with CD4 and CD8 T-cell activity that is regulated by cytolytic or noncytolytic antiviral mechanism [14]. To determine whether CD4 or CD8 T-cell activity was required for the reduction in HCV core protein levels in the livers of transgenic mice, we analyzed the core protein levels in CN2-29$^{(+/-)}$/MxCre$^{(+/-)}$ mice immunized with rVV-N25 in the absence of CD4 or CD8 T cells (Figure 4A). As expected, the mice lacking CD4 or CD8 T cells failed to show a reduction in HCV core protein levels (Figure 4B).

However, in mice lacking either CD4 or CD8 T-cells, the pathological changes associated with chronic hepatitis were resolved following rVV-N25 immunization, and the steatosis score of rVV-N25-treated mice was significantly lower than that of control mice (Figures 4C–E). These results indicated that CD4 and CD8 T cells were not responsible for the rVV-N25-induced amelioration of histological findings and that other inflammatory cell types may play an as-yet-unidentified role in the resolution of the pathological changes in these mice.

rVV-N25 Immunization Induced an NS2-specific Activated CD8 T cells Response

Because we found that HCV protein reduction in the liver required CD8 T cells, we tested whether HCV-specific CD8 T cells were present in splenocytes 28 days after immunization. To determine the functional reactivity of HCV-specific CD8$^+$ T cells, we performed a CD107a mobilization assay and intracellular IFN-γ staining. CN2-29 transgenic mice expressed the HCV structural protein and the NS2 region. However, rVV-N25 comprised only

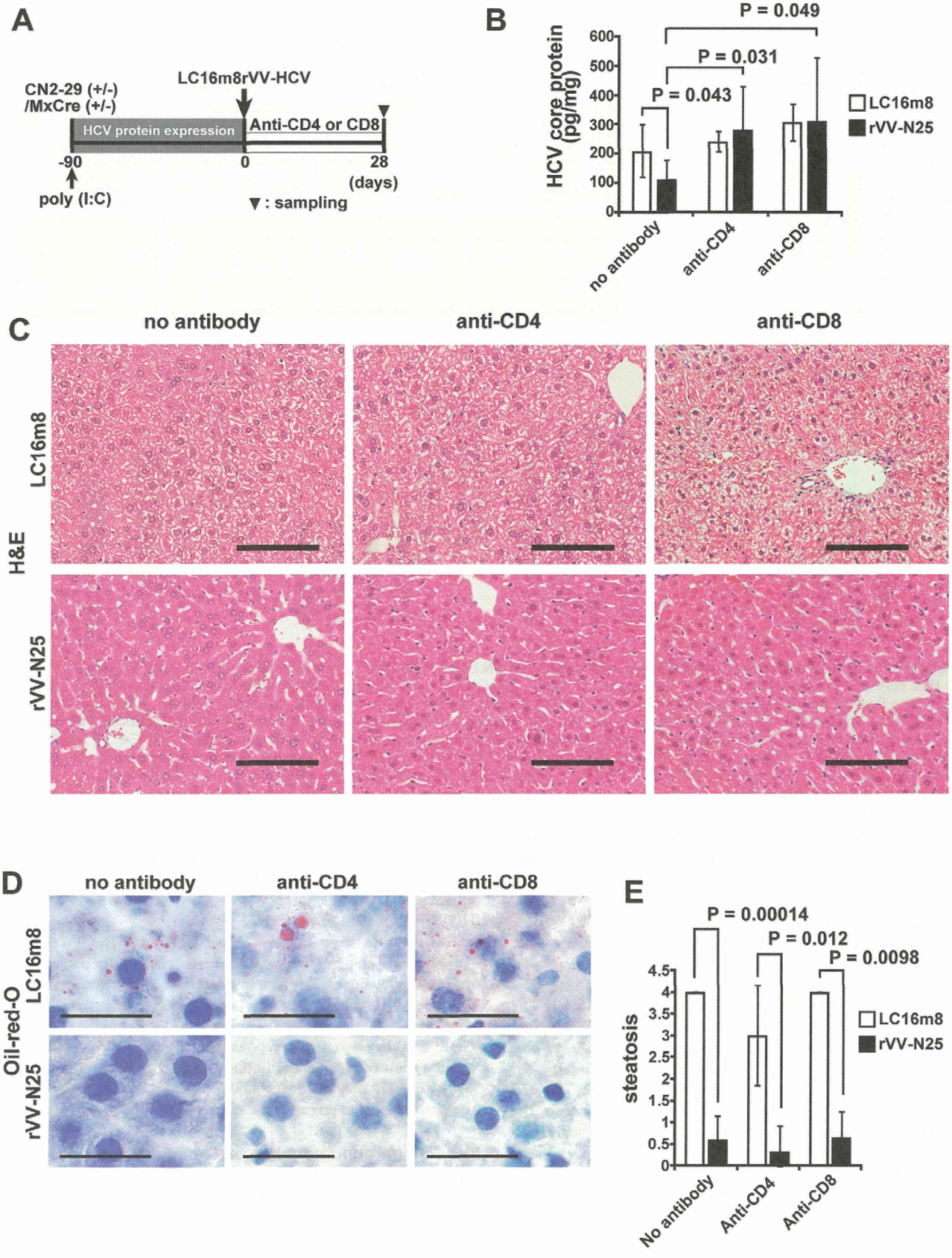

Figure 4. Role of CD4 and CD8 T cells in rVV-N25-treated mice. (**A**) Schematic diagram depicts depletion of CD4 and CD8 T cells via treatment with monoclonal antibodies. (**B**) Comparison of HCV core protein expression in control, CD4-depleted, and CD8-depleted mice 28 days after immunization with LC16m8 or rVV-N25. (**C, D**) Histological analysis of liver samples from CD4-depleted or CD8-depleted CN2-29$^{(+/-)}$/MxCre$^{(+/-)}$ mice

28 days after immunization with LC16m8 or rVV-N25. The scale bars indicate 100 μm (**C**) and 50 μm (**D**). (**E**) Histological evaluation of steatosis in liver samples from CD4-depleted or CD8-depleted CN2-29$^{(+/-)}$/MxCre$^{(+/-)}$ mice 28 days after immunization with LC16m8 or rVV-N25. Significant relationships are indicated by a P-value.
doi:10.1371/journal.pone.0051656.g004

a HCV nonstructural protein. Thus, we focused on the role of the NS2 region as the target for CD8 T cells and generated EL-4 cell lines that expressed the NS2 antigen or the CN2 antigen.

Isolated splenocytes from immunized mice were co-cultured with EL-4CN2 or EL-4NS2 cell lines for 2 weeks and analyzed.

Cytolytic cell activation can be measured using CD107a, a marker of degranulation [15]. The ratio of CD8$^+$CD107a$^+$ cells to all CD8 T cells significantly increased in rVV-N25-treated splenocytes after co-culture with EL-4CN2 or EL-4NS2 ($P<0.05$), whereas splenocytes that had been treated with any other rVV were not detected (Figure 5A, B and C). These results indicated that rVV-N25 treatment increased the frequency of HCV NS2-specific activated CD8 T cells. Consistent with these results, the ratio of CD8$^+$IFN-γ$^+$ cells to all CD8 T cells for rVV-N25-treated mice was also significantly higher than that for mice treated with any other rVV ($P<0.05$). Taken together, these findings indicated that rVV-N25 induced an effective CD8 T-cell immune response and that NS2 is an important epitope for CD8 T cells.

rVV-N25 Immunization Suppressed Inflammatory Cytokines Production

To determine whether rVV-N25 treatment affected inflammatory cytokine production, we measured serum levels of inflammatory cytokines after rVV immunization. The serum levels of these inflammatory cytokines increased in the CN2-29$^{(+/-)}$/MxCre$^{(+/-)}$ mice (Figure 6A, Figure S5). Immunization with rVV-N25 affected serum levels of inflammatory cytokines in CN2-29$^{(+/-)}$/MxCre$^{(+/-)}$ mice and caused a return to the cytokine levels observed in wild-type untreated mice (Figure 6A). In wild-type mice, the cytokine levels remained unchanged after immunization (Figure 6A). These results indicated that inflammatory cytokines were responsible for liver pathogenesis in the transgenic mice.

To test the hypothesis that inflammatory cytokines were responsible for liver pathogenesis in CN2-29$^{(+/-)}$/MxCre$^{(+/-)}$ mice, we administered transgenic mouse serum intravenously into nontransgenic mice. We observed the development of chronic hepatitis in the nontransgenic mice within 7 days after the serum transfer (Figures 6B and C). This finding was consistent with the

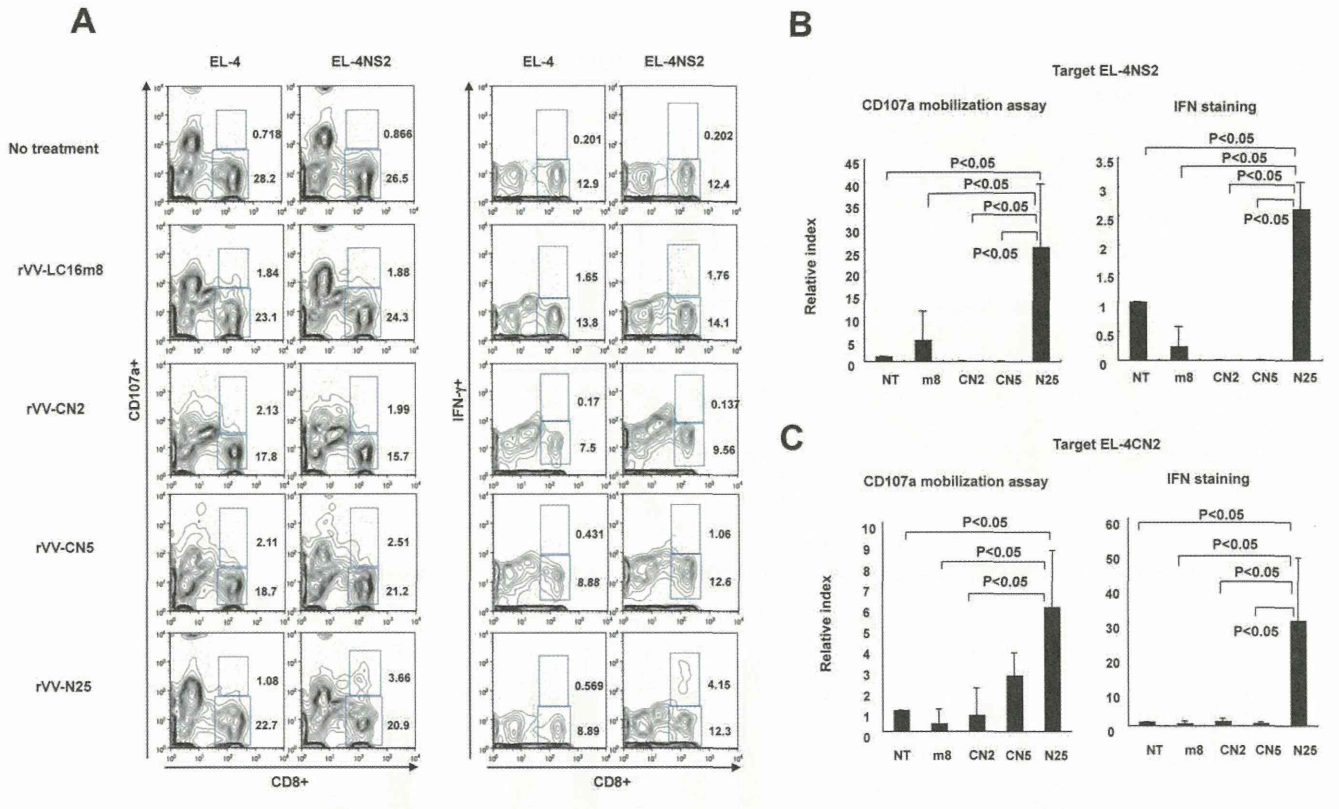

Figure 5. Immunization with rVV-N25 induced CD8 T-cell degranulation, a marker for cytotoxicity, and IFN-γ production. (**A**) The numbers represent the percentage of CD107a positive cells and negative cells (left two columns) and IFN-γ-positive cells and negative cells (right two columns). (**B, C**) The ratio of CD8$^+$IFN-γ$^+$ cells to all CD8 T cells for rVV-N25-treated mice was significantly higher than that for mice treated with any other rVV. Splenocytes (4×10^6 per well) were cultured with EL-4CN2 or EL-4NS2 cell lines in RPMI 1640 complete medium including 3% T-STIM^{TM} with ConA for 2 weeks. Harvested cells were incubated for 4 h with EL-4, EL-4CN2, or EL-4NS2 in combination with PE-labeled anti-CD107a mAb and monensin in RPMI 1640 complete medium with 50 IU/mL IL-2, according to the manufacturer's instruction. After incubation, cell suspensions were washed with PBS, and the cells were further stained with APC-labeled anti-IFN-γ mAb and Pacific blue-labeled anti-CD8 mAb. Harvested cells were stained with anti-CD107a-PE, anti-IFN-γ-APC, or anti-CD8-Pacific blue. Results that are representative of three independent experiments are shown. Significant relationships are indicated by P-value.
doi:10.1371/journal.pone.0051656.g005

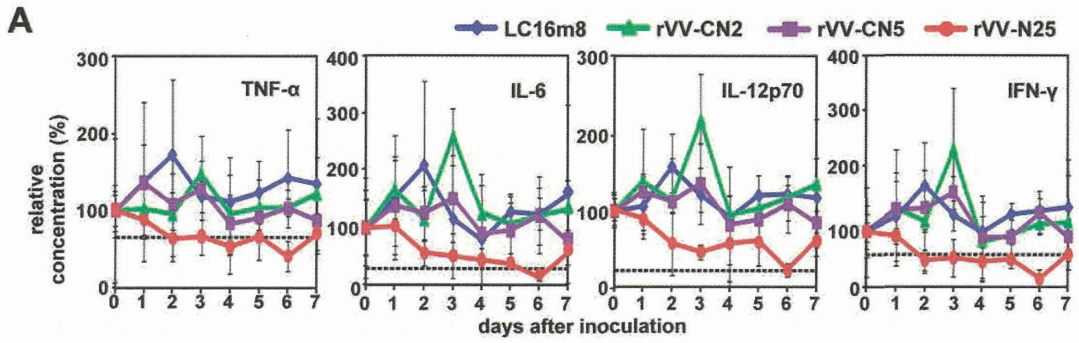
A
LC16m8
rVV-CN2
rVV-CN5
rVV-N25
TNF-α
IL-6
IL-12p70
IFN-γ
relative concentration (%)
days after inoculation

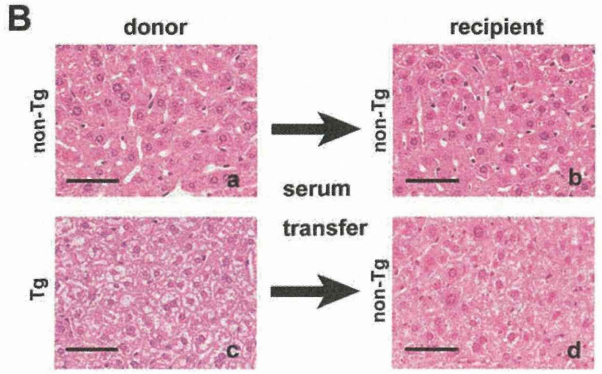
B
donor
recipient
non-Tg
Tg
serum transfer
a
b
c
d

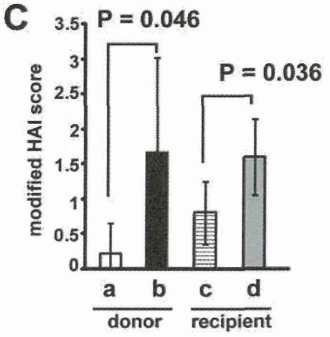
C
P = 0.046
P = 0.036
modified HAI score
a b c d
donor
recipient

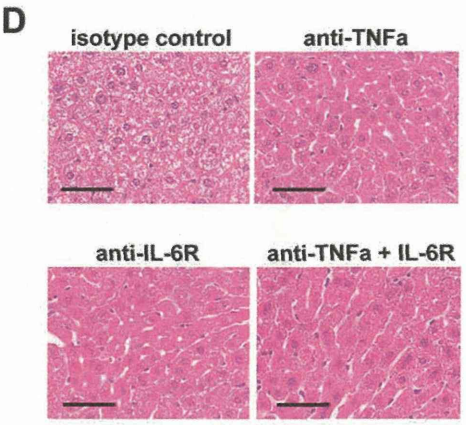
D
isotype control
anti-TNFa
anti-IL-6R
anti-TNFa + IL-6R

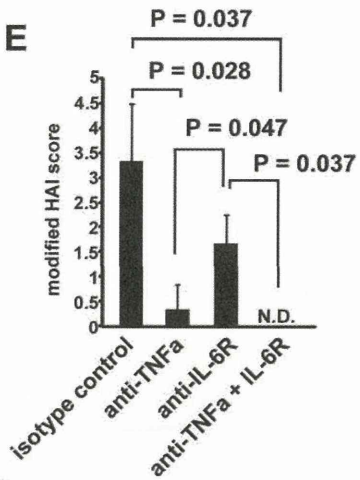
E
P = 0.037
P = 0.028
P = 0.047
P = 0.037
modified HAI score
N.D.
isotype control
anti-TNFa
anti-IL-6R
anti-TNFa + IL-6R

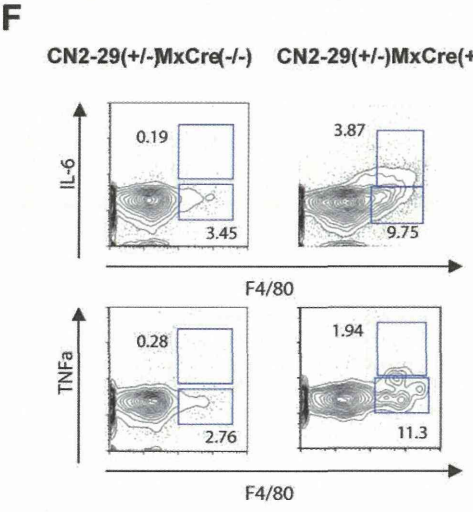
F
CN2-29(+/-)MxCre(-/-)
CN2-29(+/-)MxCre(+/-)
IL-6
TNFa
F4/80
0.19
3.45
3.87
9.75
0.28
2.76
1.94
11.3

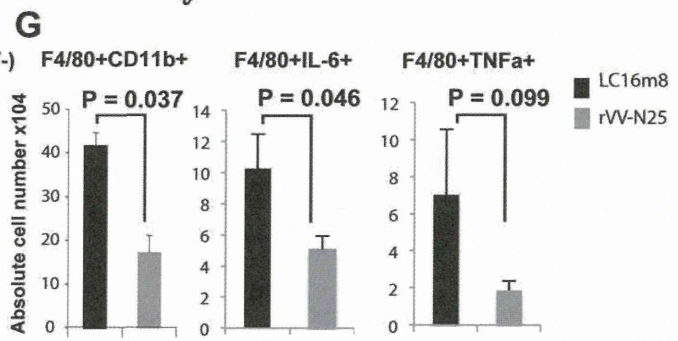
G
F4/80+CD11b+
F4/80+IL-6+
F4/80+TNFa+
P = 0.037
P = 0.046
P = 0.099
Absolute cell number x104
LC16m8
rVV-N25

Figure 6. Immunization with rVV-N25 suppresses serum inflammatory cytokine levels. (**A**) Daily cytokine levels in the serum of CN2-29$^{(+/-)}$/MxCre$^{(+/-)}$ mice during the week following immunization with LC16m8, rVV-CN2, rVV-N25, or rVV-CN5. Values represent means ± SD (n = 3) and reflect the concentrations relative to those measured on day 0. The broken lines indicate the baseline data from wild-type mice. In all cases, n = 6 mice per group. (**B**) Liver sections from CN2-29$^{(+/-)}$/MxCre$^{(+/-)}$ and CN2-29$^{(+/-)}$/MxCre$^{(-/-)}$ mice. (**C**) Histology activity index (HAI) scores of liver samples taken from CN2-29$^{(+/-)}$/MxCre$^{(+/-)}$, or CN2-29$^{(+/-)}$/MxCre$^{(-/-)}$ mice. (**D**) Liver sections from CN2-29$^{(+/-)}$/MxCre$^{(+/-)}$ mice in which TNF-α was neutralized and the IL-6 receptor was blocked. The scale bars indicate 50 μm. (**E**) HAI scores of liver samples taken from CN2-29$^{(+/-)}$/MxCre$^{(+/-)}$ in which TNF-α was neutralized and the IL-6 receptor was blocked. Tg and non-Tg indicate CN2-29$^{(+/-)}$/MxCre$^{(+/-)}$ and CN2-29$^{(+/-)}$/MxCre$^{(-/-)}$, respectively. (F) Macrophages were the main producers of TNF-α and IL-6 in CN2-29$^{(+/-)}$/MxCre$^{(+/-)}$ mice following poly(I:C) injection. (G) Immunization with rVV-N25 reduced the number of macrophages in liver samples from CN2-29$^{(+/-)}$/MxCre$^{(+/-)}$ mice and suppressed TNF-α and IL-6 production from macrophages (Figure 6G). Significant relationships are indicated by a P-value.
doi:10.1371/journal.pone.0051656.g006

hypothesis that inflammatory mediators played a key role in inducing hepatitis. Furthermore, to investigate whether TNF-α and IL-6 played particularly critical roles in the pathogenesis of chronic hepatitis in the transgenic mice, we neutralized TNF-α and blocked the IL-6 receptor in the livers of these mice. As expected, chronic hepatitis did not develop in these mice. (Figure 6D and E).

Next, to determine which cell population(s) produced TNF-α, IL-6, or both during continuous HCV expression in CN2-29$^{(+/-)}$/MxCre$^{(+/-)}$ mice, we isolated intrahepatic lymphocytes (IHLs) and labeled the macrophages (the F4/80^{+} cells) with anti-TNF-α and anti-IL-6 antibodies using an intracellular cytokine detection method. Macrophages in CN2-29$^{(+/-)}$/MxCre$^{(-/-)}$ mice produced small amounts of TNF-α and IL-6, while those in CN2-29$^{(+/-)}$/MxCre$^{(+/-)}$ mice produced much larger amounts of these cytokines (Figure 6F).

Finally, we evaluated whether rVV-N25 treatment affected the number of macrophages, cytokine production by macrophages, or both; specifically, we isolated IHLs from CN2-29$^{(+/-)}$/MxCre$^{(+/-)}$ mice 7 days after immunization with rVV-N25 or with LC16m8. The percentage of macrophages (CD11b^{+}F4/80^{+}) among IHLs and IL-6 production from these macrophages were significantly lower in rVV-N25-treated mice than in control mice (Figure 6G). Though the percentage of TNF-α-producing macrophages was not significantly different in rVV-N25-treated and control mice (P = 0.099), rVV-N25 treatment appeared to suppress these macrophages. These results demonstrated that rVV-N25 had a suppressive effect on activated macrophages, and they indicated that this suppression ameliorated the histological indicators of chronic hepatitis.

Discussion

Various HCV transgenic mouse models have been developed and used to examine immune response to HCV expression and the effects of pathogenic HCV protein on hepatocytes [4,16,17]. However, these transgenic mice develop tolerance to the HCV protein; therefore, examining immune response to HCV protein has been difficult.

To overcome the problem of immune tolerance in mouse models of HCV expression, we developed an HCV model in mice that relies on conditional expression of the core, E1, E2, and NS2 proteins and the Cre/loxP switching system [5,6]; we showed that the injection of an Ad-Cre vector enhanced the frequency of HCV-specific activated CD8 T cells in the liver of these mice and caused liver injury. However, the Ad-Cre adenovirus vector alone causes acute hepatitis in wild-type mice. Nevertheless, the transgenic model was useful for evaluating interactions between the host immune system and viral protein (serum ALT level over 2,000 IU/L) [5]; HCV core protein levels were reduced and expression of this protein was transient (about 2 weeks). Therefore, this Ad-Cre-dependent model cannot be used to effectively investigate immune responses to chronic HCV hepatitis.

Here, we used poly (I:C)-induced expression of Cre recombinase to generate HCV transgenic mice in order to study the effect of HCV protein and confirmed that these mice developed chronic active hepatitis–including steatosis, lipid deposition, and hepatocellular carcinoma. These pathological findings in the transgenic mice were very similar to those in humans with chronic hepatitis C; therefore, this mouse model of HCV may be useful for analyzing the immune response to chronic hepatitis. However, experimental results obtained with this mouse model may not directly translate to clinical findings from patients with HCV infection because the expression of HCV proteins was not liver specific in these mice. Furthermore, poly(I:C) injection can activate innate immune responses and, consequently, might induce temporary liver injury [18]. Additionally, poly(I:C) injection has an adjuvant effect; specifically, it stimulates TLR3 signaling [19].

To evaluate whether poly(I:C) injection caused hepatitis in CN2-29$^{(+/-)}$/MxCre$^{(-/-)}$ mice, we examined serum ALT levels and liver histology following poly(I:C) injection. We found that, following poly(I:C) injection, serum ALT levels in CN2-29$^{(+/-)}$/MxCre$^{(-/-)}$ mice increased, reached a peak one day after injection, declined from day 1 to day 6, and were not elevated thereafter; this time-course indicated that poly(I:C) injection alone did not induced continuous liver injury (figure S6). Based on these findings, we believe that the effects of poly(I:C) injection in these mice did not confound our analysis of chronic hepatitis.

Immunization with rVV-N25 suppressed HCV protein levels in the liver, and this suppression was associated with ameliorated pathological chronic hepatitis findings (see Figure 3). Importantly, rVV-N25 treatment did not cause liver injury based on the serum ALT levels; therefore, this treatment was unlikely to have cytopathic effects on infected hepatocytes. These findings provided strong evidence that rVV-N25 treatment effectively halted the progression of chronic hepatitis. Immunization with plasmid DNA or with recombinant vaccinia virus can effectively induce cellular and humoral immune responses and exert a protective effect against challenge with HCV infection [20,21]. However, findings from these previous studies revealed HCV immunization of both uninfected, naïve animals and immune-tolerant animals induced a HCV-specific immune response. In the model describe here; the animals were immune competent for HCV; therefore, our findings provided further important evidence that rVV-N25 was effective in the treatment of chronic hepatitis.

In addition, we demonstrated that rVV-N25 treatment in the absence of CD4 and CD8 T cells had no effect on HCV clearance. This important observation indicated that rVV-N25-induced HCV clearance was mediated by CD4 and CD8 T cells. Many studies have shown that spontaneous viral clearance during acute HCV infection is characterized by a vigorous, broadly reactive CD4 and CD8 T-cell response. [8,22] HCV clearance and hepatocellular cytotoxicity are both mediated by CD8 antigen-specific (cytotoxic T lymphocyte) CTLs [23]. Consistent with these observations, rVV-N25 treatment effectively induced the accumulation of NS2-specific CD8 T cells, which express high levels of

CD107a and IFN-γin the spleen. Notably, even with rVV-N25 immunization, the frequency of activated CD8 T cells was very low, and a minimum of 2-weeks incubation was required to distinguish the difference between rVV treatments. Even if a small population of specific CD8+ T cells played a relevant role in the reduction of core protein, it is difficult to assert that the only NS2-specific CD8+ T cells were important to this reduction. However, based on the results presented in Figure 4B, we are able to conclude that at least CD8+ and/or CD4+ T cells were important to the reduction in HCV core protein. Therefore, to elucidate the mechanism of HCV protein clearance, further investigation of not only the other T cell epitopes but also other immunocompetent cells is required.

Interestingly, rVV-N25 treatment–but not the rVV-CN2 or rVV-CN5 treatment–efficiently induced a HCV-specific activated CD8 T cells response; this difference in efficacy could have one or more possible causes. The HCV structural proteins (core, E1, and E2 proteins) in the rVV-CN construct may cause the difference; Saito et al. reported that injection with plasmid constructs encoding the core protein induced a specific CTL response in BALB/c mice [24]. Reportedly, CTL activity against core or envelope protein is completely absent from transgenic mice immunized with a plasmid encoding the HCV structural proteins, but core-specific CTL activity is present in transgenic mice that were immunized with a plasmid encoding the HCV core [21]. In contrast, when recombinant vaccinia virus expressing different regions of the HCV polyprotein were injected into BALB/c mice, only the HCV core protein markedly suppressed vaccinia-specific CTL responses [25]. Thus, the HCV core protein may have an immunomodulatory function [26]. Based on these reports and our results, we hypothesize that the causes underlying the effectiveness of rVV-N25 treatment were as follows: 1) this rVV construct included the core and envelope proteins and 2) the core protein had an immune-suppressive effect on CTL induction. Therefore, we suggest that exclusion of the core and envelope antigen as immunogen is one important factor in HCV vaccine design.

Interestingly, immunization with rVV-N25 rapidly suppressed the inflammatory response; however, immunization with either of the other rVVs did not (see Figure 6A). This result indicated that rVV-N25 may modulate inflammation via innate immunity, as well as via acquired immunity. Reportedly, Toll-like receptor (TLR)-dependent recognition pathways play a role in the recognition of poxviruses [27]. TLR2 and TLR9 have also been implicated in the recognition of the vaccinia virus [28,29]. These findings indicate that TLR on dendritic cells may modulate the immunosuppressive effect of rVV-N25 in our model of HCV infection; however, further examination of this hypothesis is required. The finding that pathological symptoms in the HCV transgenic mice were completely blocked by intravenous injection of TNF-α and IL-6 neutralizing antibodies indicated that the progression of chronic hepatitis depended on inflammatory cytokines in serum, rather than the HCV protein levels in hepatocytes. Lymphocytes, macrophages, hepatocytes, and adipocytes each produce TNF-α and IL-6 [30,31], and HCV-infected patients have elevated levels of TNF-α and IL-6 [32,33]. Both cytokines also contribute to the maintenance of hepatosteatosis in mice fed a high-fat diet [34], and production of TNF-α and IL-6 is elevated in obese mice due to the low grade inflammatory response that is caused by lipid accumulation [35]. These findings indicate that both cytokines are responsible for HCV-triggered hepatosteatosis, and anti-cytokine neutralization is a potential treatment for chronic hepatitis if antiviral therapy is not successful.

The reduction of macrophages in number might be due to the induction of apoptosis by vaccinia virus *in vitro* infection as previous reported [36]. To understand the mechanisms responsible for the reduction of the number of macrophage, we performed another experiment to confirm whether the macrophages were infected with vaccinia virus inoculation. However, based on PCR analyses; vaccinia virus DNA was not present in liver tissue that contained macrophages (Figure S7). Furthermore, apoptosis of macrophages was not detected in liver samples (Data not shown). Based on these results, it is unlikely that the reduction in the number of macrophages was due to apoptosis induced by vaccinia virus infection. Although rVV-N25 reduced the number of macrophage, precise mechanism is still unknown. Further examination to elucidate the mechanism is required.

In conclusion, our findings demonstrated that rVV-N25 is a promising candidate for an HCV vaccine therapy. Additionally, the findings of this study indicate that rVV-N25 immunization can be used for prevention of HCV infection and as an antiviral therapy against ongoing HCV infection.

Materials and Methods

Ethics Statement

All animal care and experimental procedures were performed according to the guidelines established by the Tokyo Metropolitan Institute of Medical Science Subcommittee on Laboratory Animal Care; these guidelines conform to the Fundamental Guidelines for Proper Conduct of Animal Experiment and Related Activities in Academic Research Institutions under the jurisdiction of the Ministry of Education, Culture, Sports, Science and Technology, Japan, 2006. All protocols were approved by the Committee on the Ethics of Animal Experiments of the Tokyo Metropolitan Institute of Medical Science (Permit Number: 11–078). All efforts were made to minimize the suffering of the animals.

Animals

R6CN2 HCV cDNA (nt 294–3435) [37] and full genomic HCV cDNA (nt 1–9611) [38,39] were cloned from a blood sample taken from a patient (#R6) with chronic active hepatitis (Text S1). The infectious titer of this blood sample has been previously reported [40]. R6CN2HCV and R6CN5HCV transgenic mice were bred with Mx1-Cre transgenic mice (purchased from Jackson Laboratory) to produce R6CN2HCV-MxCre and R6CN5HCV-MxCre transgenic mice, which were designated CN2-29$^{(+/-)}$/MxCre$^{(+/-)}$ and RzCN5-15$^{(+/-)}$/MxCre$^{(+/-)}$ mice, respectively. Cre expression in the livers of these mice was induced by intraperitoneal injection of polyinosinic acid–polycytidylic acid [poly(I:C)] (GE Healthcare UK Ltd., Buckinghamshire, England); 300 μL of a poly(I:C) solution (1 mg/mL in phosphate-buffered saline [PBS]) was injected three times at 48-h intervals. All animal care and experimental procedures were performed according to the guidelines established by the Tokyo Metropolitan Institute of Medical Science Subcommittee on Laboratory Animal Care.

Histology and Immunohistochemical Staining

Tissue samples were fixed in 4% paraformaldehyde in PBS, embedded in paraffin, sectioned (4-μm thickness), and stained with hematoxylin and eosin (H&E). Staining with periodic acid–Schiff stain, Azan stain, silver, or Oil-red-O was also performed to visualize glycogen degeneration, fibrillization, reticular fiber degeneration, or lipid degeneration, respectively.

For immunohistochemical staining, unfixed frozen liver sections were fixed in 4% paraformaldehyde for 10 min and then incubated with blocking buffer (1% bovine serum albumin in PBS) for 30 min at room temperature. Subsequently, the sections were incubated with biotinylated mouse anti-HCV core mono-

clonal antibody (5E3) for 2 h at room temperature. After being washed with PBS, the sections were incubated with streptavidin–Alexa Fluor 488 (Invitrogen). The nuclei were stained with 4',6-diamidino-2-phenylindole (DAPI). Fluorescence was observed using a confocal laser microscope (Laser scanning microscope 510, Carl Zeiss).

Generation of rVVs

The pBR322-based plasmid vector pBMSF7C contained the ATI/p7.5 hybrid promoter within the hemagglutinin gene region of the vaccinia virus, which was reconstructed from the pSFJ1-10 plasmid and pBM vector [41,42]. Separate full-length cDNAs encoding either the HCV structural protein, nonstructural protein, or all HCV proteins were cloned from HCV R6 strain (genotype 1b) RNA by RT-PCR. Each cDNA was inserted into a separate pBMSF7C vector downstream of the pBMSF7C ATI/p7.5 hybrid promoter; the final designation of each recombinant plasmid was pBMSF7C-CN2, pBMSF7C-N25, or pBMSF-CN5 (Figure 2). They were then transfected into primary rabbit kidney cells infected with LC16m8 (multiplicity of infection = 10). The virus–cell mixture was harvested 24 h after the initial transfection by scrapping; the mixture was then frozen at −80°C until use. The hemagglutinin-negative recombinant viruses were cloned as previously described [42] and named rVV-CN2, rVV-N25, or rVV-CN5. Insertion of the HCV protein genes into the LC16m8 genome was confirmed by direct PCR, and expression of each protein from the recombinant viruses was confirmed by western blot analysis. The titers of rVV-CN2, rVV-N25, and rVV-CN5 were determined using a standard plaque assay and RK13 cells.

Statistical Analysis

Data are shown as mean ± SD. Data were analyzed using the nonparametric Mann–Whitney or Kruskal–Wallis tests or ANOVA as appropriate; GraphPad Prism 5 for Macintosh (GraphPad) was used for all analyses. P values <0.05 were considered statistically significant.

Supporting Information

Figure S1 HAI score of liver samples taken from CN2-29$^{(+/-)}$/MxCre$^{(+/-)}$ mice.
(EPS)

Figure S2 Lipid degeneration in samples of liver taken from CN2-29$^{(+/-)}$/MxCre$^{(+/-)}$ mice.
(EPS)

Figure S3 HCV protein expression after infection of LC16m8, rVV-CN2, rVV-N25, or rVV-CN5 into HepG2 cells.
(EPS)

Figure S4 Effects of treatment with rVV-N25 in RzCN5-15$^{(+/-)}$/MxCre$^{(+/-)}$ mice.
(EPS)

Figure S5 Daily cytokine profiles of the serum from CN2-29$^{(+/-)}$/MxCre$^{(+/-)}$ mice during the week following inoculation with LC16m8, rVV-CN2, rVV-N25, or rVV-CN5.
(EPS)

Figure S6 The immune response following poly(I:C) injection in the acute phase.
(EPS)

Figure S7 Detection of vaccinia virus DNA in the skin, liver, and spleen after inoculation with attenuated vaccinia virus (Lister strain) or highly attenuated vaccinia virus (LC16m8 strain).
(EPS)

Table S1 Incidence of hepatocellular carcinoma in male and female transgenic mice at 360, 480, and 600 days after poly(I:C) injection.
(EPS)

Text S1 Supporting information including material and methods, and references.
(DOCX)

Acknowledgments

We thank Dr. Fukashi Murai for supporting this study. We also thank Dr. Keiji Tanaka for providing the MxCre mice, Dr. Shigeo Koyasu for providing the GK1.5 (anti-CD4) and 53–6.72 (anti-CD8) monoclonal antibodies, and Dr Takashi Tokuhisa for helpful discussions.

Author Contributions

Performed the experiments: SS KK TC Y. Tobita TO FY Y. Tokunaga. Analyzed the data: SS KK TC MK. Contributed reagents/materials/analysis tools: KT-K TW TT MM K. Mizuno YH TH K. Matsushima. Wrote the paper: SS KK MK. Study concept and design: MK.

References

1. Lauer GM, Walker BD (2001) Hepatitis C virus infection. N Engl J Med 345: 41–52.
2. Alter MJ (1995) Epidemiology of hepatitis C in the West. Semin Liver Dis 15: 5–14.
3. Kawamura T, Furusaka A, Koziel MJ, Chung RT, Wang TC, et al. (1997) Transgenic expression of hepatitis C virus structural proteins in the mouse. Hepatology 25: 1014–1021.
4. Moriya K, Fujie H, Shintani Y, Yotsuyanagi H, Tsutsumi T, et al. (1998) The core protein of hepatitis C virus induces hepatocellular carcinoma in transgenic mice. Nat Med 4: 1065–1067.
5. Wakita T, Katsume A, Kato J, Taya C, Yonekawa H, et al. (2000) Possible role of cytotoxic T cells in acute liver injury in hepatitis C virus cDNA transgenic mice mediated by Cre/loxP system. J Med Virol 62: 308–317.
6. Wakita T, Taya C, Katsume A, Kato J, Yonekawa H, et al. (1998) Efficient conditional transgene expression in hepatitis C virus cDNA transgenic mice mediated by the Cre/loxP system. J Biol Chem 273: 9001–9006.
7. Folgori A, Capone S, Ruggeri L, Meola A, Sporeno E, et al. (2006) A T-cell HCV vaccine eliciting effective immunity against heterologous virus challenge in chimpanzees. Nat Med 12: 190–197.
8. Chisari FV, Ferrari C (1995) Hepatitis B virus immunopathology. Springer Semin Immunopathol 17: 261–281.
9. Machida K, Tsukiyama-Kohara K, Seike E, Tone S, Shibasaki F, et al. (2001) Inhibition of cytochrome c release in Fas-mediated signaling pathway in transgenic mice induced to express hepatitis C viral proteins. J Biol Chem 276: 12140–12146.
10. Kuhn R, Schwenk F, Aguet M, Rajewsky K (1995) Inducible gene targeting in mice. Science 269: 1427–1429.
11. Li K, Chen Z, Kato N, Gale M Jr, Lemon SM (2005) Distinct poly(I-C) and virus-activated signaling pathways leading to interferon-beta production in hepatocytes. J Biol Chem 280: 16739–16747.
12. Sugimoto M, Yamanouchi K (1994) Characteristics of an attenuated vaccinia virus strain, LC16m0, and its recombinant virus vaccines. Vaccine 12: 675–681.
13. Youn JW, Hu YW, Tricoche N, Pfahler W, Shata MT, et al. (2008) Evidence for protection against chronic hepatitis C virus infection in chimpanzees by immunization with replicating recombinant vaccinia virus. J Virol 82: 10896–10905.
14. Guidotti LG, Rochford R, Chung J, Shapiro M, Purcell R, et al. (1999) Viral clearance without destruction of infected cells during acute HBV infection. Science 284: 825–829.
15. Burkett MW, Shafer-Weaver KA, Strobl S, Baseler M, Malyguine A (2005) A novel flow cytometric assay for evaluating cell-mediated cytotoxicity. J Immunother 28: 396–402.

16. Pasquinelli C, Shoenberger JM, Chung J, Chang KM, Guidotti LG, et al. (1997) Hepatitis C virus core and E2 protein expression in transgenic mice. Hepatology 25: 719–727.
17. Lerat H, Honda M, Beard MR, Loesch K, Sun J, et al. (2002) Steatosis and liver cancer in transgenic mice expressing the structural and nonstructural proteins of hepatitis C virus. Gastroenterology 122: 352–365.
18. Lang KS, Georgiev P, Recher M, Navarini AA, Bergthaler A, et al. (2006) Immunoprivileged status of the liver is controlled by Toll-like receptor 3 signaling. The Journal of clinical investigation 116: 2456–2463.
19. Jasani B, Navabi H, Adams M (2009) Ampligen: a potential toll-like 3 receptor adjuvant for immunotherapy of cancer. Vaccine 27: 3401–3404.
20. Elmowalid GA, Qiao M, Jeong SH, Borg BB, Baumert TF, et al. (2007) Immunization with hepatitis C virus-like particles results in control of hepatitis C virus infection in chimpanzees. Proc Natl Acad Sci U S A 104: 8427–8432.
21. Satoi J, Murata K, Lechmann M, Manickan E, Zhang Z, et al. (2001) Genetic immunization of wild-type and hepatitis C virus transgenic mice reveals a hierarchy of cellular immune response and tolerance induction against hepatitis C virus structural proteins. J Virol 75: 12121–12127.
22. Crispe IN (2009) The liver as a lymphoid organ. Annu Rev Immunol 27: 147–163.
23. Chisari FV (2005) Unscrambling hepatitis C virus-host interactions. Nature 436: 930–932.
24. Saito T, Sherman GJ, Kurokohchi K, Guo ZP, Donets M, et al. (1997) Plasmid DNA-based immunization for hepatitis C virus structural proteins: immune responses in mice. Gastroenterology 112: 1321–1330.
25. Large MK, Kittlesen DJ, Hahn YS (1999) Suppression of host immune response by the core protein of hepatitis C virus: possible implications for hepatitis C virus persistence. Journal of immunology 162: 931–938.
26. Dustin LB, Rice CM (2007) Flying under the radar: the immunobiology of hepatitis C. Annu Rev Immunol 25: 71–99.
27. Bowie A, Kiss-Toth E, Symons JA, Smith GL, Dower SK, et al. (2000) A46R and A52R from vaccinia virus are antagonists of host IL-1 and toll-like receptor signaling. Proc Natl Acad Sci U S A 97: 10162–10167.
28. Zhu J, Martinez J, Huang X, Yang Y (2007) Innate immunity against vaccinia virus is mediated by TLR2 and requires TLR-independent production of IFN-beta. Blood 109: 619–625.
29. Samuelsson C, Hausmann J, Lauterbach H, Schmidt M, Akira S, et al. (2008) Survival of lethal poxvirus infection in mice depends on TLR9, and therapeutic vaccination provides protection. J Clin Invest 118: 1776–1784.
30. Sheikh MY, Choi J, Qadri I, Friedman JE, Sanyal AJ (2008) Hepatitis C virus infection: molecular pathways to metabolic syndrome. Hepatology 47: 2127–2133.
31. Tilg H, Moschen AR, Kaser A, Pines A, Dotan I (2008) Gut, inflammation and osteoporosis: basic and clinical concepts. Gut 57: 684–694.
32. Malaguarnera M, Di Fazio I, Laurino A, Ferlito L, Romano M, et al. (1997) Serum interleukin 6 concentrations in chronic hepatitis C patients before and after interferon-alpha treatment. Int J Clin Pharmacol Ther 35: 385–388.
33. Larrea E, Garcia N, Qian C, Civeira MP, Prieto J (1996) Tumor necrosis factor alpha gene expression and the response to interferon in chronic hepatitis C. Hepatology 23: 210–217.
34. Park EJ, Lee JH, Yu GY, He G, Ali SR, et al. (2010) Dietary and genetic obesity promote liver inflammation and tumorigenesis by enhancing IL-6 and TNF expression. Cell 140: 197–208.
35. Gregor MF, Hotamisligil GS (2011) Inflammatory mechanisms in obesity. Annu Rev Immunol 29: 415–445.
36. Humlova Z, Vokurka M, Esteban M, Melkova Z (2002) Vaccinia virus induces apoptosis of infected macrophages. The Journal of general virology 83: 2821–2832.
37. Choo QL, Kuo G, Weiner AJ, Overby LR, Bradley DW, et al. (1989) Isolation of a cDNA clone derived from a blood-borne non-A, non-B viral hepatitis genome. Science 244: 359–362.
38. Tsukiyama-Kohara K, Tone S, Maruyama I, Inoue K, Katsume A, et al. (2004) Activation of the CKI-CDK-Rb-E2F pathway in full genome hepatitis C virus-expressing cells. J Biol Chem 279: 14531–14541.
39. Nishimura T, Kohara M, Izumi K, Kasama Y, Hirata Y, et al. (2009) Hepatitis C virus impairs p53 via persistent overexpression of 3beta-hydroxysterol Delta24-reductase. J Biol Chem 284: 36442–36452.
40. Shimizu YK, Purcell RH, Yoshikura H (1993) Correlation between the infectivity of hepatitis C virus in vivo and its infectivity in vitro. Proc Natl Acad Sci U S A 90: 6037–6041.
41. Yasui F, Kai C, Kitabatake M, Inoue S, Yoneda M, et al. (2008) Prior immunization with severe acute respiratory syndrome (SARS)-associated coronavirus (SARS-CoV) nucleocapsid protein causes severe pneumonia in mice infected with SARS-CoV. J Immunol 181: 6337–6348.
42. Kitabatake M, Inoue S, Yasui F, Yokochi S, Arai M, et al. (2007) SARS-CoV spike protein-expressing recombinant vaccinia virus efficiently induces neutralizing antibodies in rabbits pre-immunized with vaccinia virus. Vaccine 25: 630–637.

SCIENTIFIC REPORTS

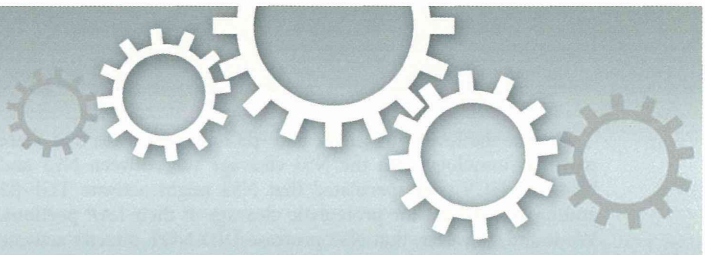

OPEN

SUBJECT AREAS:
MECHANISMS OF DISEASE
HEPATITIS C
LIVER FIBROSIS
TRANSFORMING GROWTH FACTOR BETA

Received
25 July 2013

Accepted
31 October 2013

Published
22 November 2013

Correspondence and requests for materials should be addressed to S.K. (skojima@riken.jp)

HCV NS3 protease enhances liver fibrosis via binding to and activating TGF-β type I receptor

Kotaro Sakata[1,2,3], Mitsuko Hara[1], Takaho Terada[4,5], Noriyuki Watanabe[6], Daisuke Takaya[4,7], So-ichi Yaguchi[8], Takehisa Matsumoto[4,7], Tomokazu Matsuura[9], Mikako Shirouzu[4,7], Shigeyuki Yokoyama[4,5], Tokio Yamaguchi[10], Keiji Miyazawa[8], Hideki Aizaki[6], Tetsuro Suzuki[11], Takaji Wakita[6], Masaya Imoto[2] & Soichi Kojima[1]

[1]Micro-signaling Regulation Technology Unit, RIKEN Center for Life Science Technologies, Saitama 351-0198, Japan, [2]Department of Biosciences and Informatics, Faculty of Science and Technology, Keio University, Kanagawa 223-8522, Japan, [3]Drug Discovery Laboratory, Wakunaga Pharmaceutical Co., Ltd., Hiroshima 739-1195, Japan, [4]RIKEN Systems and Structural Biology Center, Kanagawa 230-0045, Japan, [5]RIKEN Structural Biology Laboratory, Kanagawa 230-0045, Japan, [6]Department of Virology II, National Institute of Infectious Diseases, Tokyo 162-8640, Japan, [7]Division of Structural and Synthetic Biology, RIKEN Center for Life Science Technologies, Kanagawa 230-0045, Japan, [8]Department of Biochemistry, Interdisciplinary Graduate School of Medicine and Engineering, University of Yamanashi, Yamanashi 409-3898, Japan, [9]Department of Laboratory Medicine, the Jikei University School of Medicine, Tokyo 105-8461, Japan, [10]RIKEN Program for Drug Discovery and Medical Technology Platforms, Saitama 351-0198, Japan, [11]Department of Infectious Diseases, Hamamatsu University School of Medicine, Shizuoka 431-3192, Japan.

Viruses sometimes mimic host proteins and hijack the host cell machinery. Hepatitis C virus (HCV) causes liver fibrosis, a process largely mediated by the overexpression of transforming growth factor (TGF)-β and collagen, although the precise underlying mechanism is unknown. Here, we report that HCV non-structural protein 3 (NS3) protease affects the antigenicity and bioactivity of TGF-β2 in $(CAGA)_9$-Luc CCL64 cells and in human hepatic cell lines via binding to TGF-β type I receptor (TβRI). Tumor necrosis factor (TNF)-α facilitates this mechanism by increasing the colocalization of TβRI with NS3 protease on the surface of HCV-infected cells. An anti-NS3 antibody against computationally predicted binding sites for TβRI blocked the TGF-β mimetic activities of NS3 *in vitro* and attenuated liver fibrosis in HCV-infected chimeric mice. These data suggest that HCV NS3 protease mimics TGF-β2 and functions, at least in part, via directly binding to and activating TβRI, thereby enhancing liver fibrosis.

Viruses sometimes take over the host cell machinery by mimicking host cell proteins. This strategy infers survival, infection, and replication advantages to the virus[1,2], which may thereby contribute to the development of human disease.

Chronic hepatitis C virus (HCV) infection is one of the major causes of liver fibrosis, cirrhosis, and hepatocellular carcinoma[3,4]. However, the molecular mechanism by which HCV induces liver fibrosis is not fully understood. An estimated 130–170 million people worldwide are infected with HCV[5]. HCV, classified in the genus *Hepacivirus* of the family *Flaviviridae*, is a positive-strand RNA virus with an approximately 9.6-kb viral genome encoding structural (core, E1, and E2) and non-structural proteins (p7, NS2, NS3, NS4A, NS4B, NS5A, and NS5B)[6]. Of these proteins, NS3 is a member of the serine protease family that cleaves the HCV polyprotein to generate mature viral proteins that are required for viral replication[7].

Liver fibrosis, a common feature of chronic liver diseases, is caused by the excessive accumulation of extracellular matrix (ECM) proteins, including collagen. Transforming growth factor (TGF)-β, the most potent fibrogenic cytokine, is produced in its high molecular weight latent form and partly activated through the proteolytic cleavage of its propeptide region, termed latency associated protein (LAP), by serine proteases, plasmin, and plasma kallikrein[8,9]. The resultant active TGF-β signals via TGF-β type I (TβRI) and type II receptors (TβRII), inducing the phosphorylation of Smad2/3, which then binds to Smad4 and forms a complex that enters the cell nucleus. This complex acts as a transcription factor that controls the expression of target genes, including collagen and TGF-β itself, by binding to the DNA elements containing the minimal Smad-binding element, CAGA box[10].

Because the LAPs of TGF-β2 and -β3 have sequences that share partially homology with the NS3 cleavage site between NS3 and NS4A of HCV[7], we speculated that NS3 might activate TGF-β2 and/or TGF-β3 via the proteolytic cleavage of their LAP portions. We found, however, that NS3 protease DID NOT directly activate latent TGF-β2/3. Instead, it mimicked TGF-β2 and induced TGF-β signaling by binding and activating TβRI, leading to the induction of fibrogenic genes. This pathway was enhanced in the presence of an inflammatory cytokine, tumor necrosis factor (TNF)-α, as TNF-α increased the expression of TβRI. Furthermore, we found that NS3 colocalized with TβRI on the surface of an HCV-infected hepatoma cell line, and we observed direct binding between recombinant NS3 and TβRI. These phenomena were reproduced in chimeric mice transplanted with human hepatocytes that had been infected with HCV. These data suggest a novel mechanism by which HCV induces liver fibrosis.

Results

HCV NS3 protease exerted TGF-β mimetic activity via TβRI. To confirm whether HCV NS3 protease might induce the activation of latent TGF-β2, bacterially expressed recombinant NS3 (Supplementary Fig. S1) was incubated with conditioned medium obtained from HEK293T cells transiently overexpressing latent TGF-β2, and the concentration of active TGF-β2 in the reaction mixtures were measured by ELISA. Although the addition of NS3 increased active TGF-β2 concentrations in a dose-dependent manner, these increases were not time-dependent (Supplementary Fig. S2). Instead, we found that NS3 protease itself reacted with TGF-β2 in a dose-dependent manner, as determined by ELISA (Fig. 1A). Next, to assess whether NS3 could induce the bioactivity of TGF-β via TβRI, and whether its activity was dependent on protease activity, we performed a luciferase reporter assay with the TGF-β-responsive $(CAGA)_9$-Luc reporter in CCL64 cells. NS3 demonstrated TGF-β mimetic activity, which was alleviated in the presence of TβRI kinase inhibitors (SB-431542 and LY-364947) in a dose-dependent manner (Fig. 1B). In contrast, an NS3 protease inhibitor, VX-950 (telaprevir), did not affect luciferase activity (Fig. 1B). An unrelated protein with almost the same molecular weight as NS3, HLA class II histocompatibility antigen, DM α chain (HLA-DMA), as well as a carrier-free, tag-control sample, did not exert TGF-β mimetic activity, thus demonstrating the specificity of NS3 (Supplementary Fig. S3). Additionally, an anti-TGF-β2 antibody that detected NS3 in the TGF-β2 ELISA did not inhibit luciferase activity (Supplementary Fig. S4).

NS3 stimulated collagen production in hepatic cells, which was augmented by TNF-α. We examined the effect of NS3 on the expression of TGF-β1 and collagen α1 (I) in the human hepatic stellate cell line LX-2. Treatment with NS3 for 12 hours significantly increased both TGF-β1 (1.6-fold) and collagen α1 (I) (1.4-fold) expression in these cells (Fig. 2A). On the contrary, NS3 did not affect the expression of these genes in the normal hepatic cell line Hc. The pretreatment of the cells with tumor necrosis factor-α (TNF-α) enhanced increased TGF-β1 and collagen α1 (I) expression mediated by NS3 and was also accompanied by an increase in TGF-β receptor expression (Fig. 2B). Further increases in TβRI expression were not observed by combination treatment with TNF-α, suggesting that TNF-α increased TβRI expression, which may have enhanced the TGF-β mimetic activity of NS3 in these cells. Furthermore, Smad3 phosphorylation was also induced by NS3 in Hc cells that had been pretreated with TNF-α (Fig. 2D). A similar cooperativity between TNF-α and NS3 protease was not observed in LX-2 cells (Fig. 2C).

Interaction between NS3 and TβRI on the surface of HCV-infected HCC cells. NS3 was immunostained on the surface of

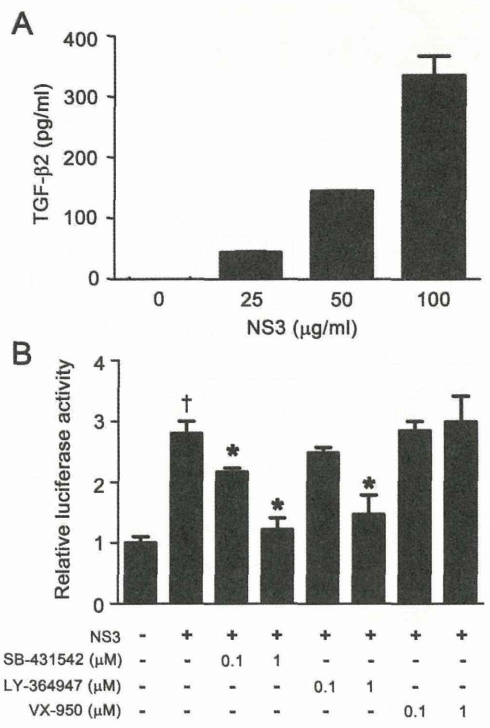

Figure 1 | HCV NS3 protease exerted TGF-β mimetic activity via the type I receptor. (A) TGF-β2 antigenicity of NS3. The indicated concentrations of recombinant NS3 protease were used in the TGF-β2 ELISA assays. (B) TGF-β mimetic activity of NS3 and its suppression by TβRI kinase inhibitors. $(CAGA)_9$-Luc CCL64 cells were stimulated with 100 μg/ml of recombinant NS3 protease for 24 hours, with or without the indicated concentration of TβRI kinase inhibitor or the NS3 protease inhibitor VX-950 (telaprevir). After 24 hours, the cells were harvested and luciferase activity measured. $\dagger p < 0.05$ compared with untreated control cells, $*p < 0.05$ compared with NS3-treated cells without any inhibitors. The data are shown as the mean ± SD (n = 3), and representative results from three independent experiments with similar results are shown.

HCV-infected Huh-7.5.1 cells both with and without permeabilization. In contrast, an ER marker, calnexin, was only positive after the permeabilization of the cells (Fig. 3A). To examine whether NS3 that was localized to the surface of HCV-infected Huh-7.5.1 cells interacted with TβRI, we performed co-immunostaining (Fig. 3B) and in situ proximity ligation assay (PLA) (Fig. 3C) using antibodies against NS3 and TβRI. Both results showed that NS3 was colocalized and formed a complex with TβRI on the cell surface. Because LX-2 cells (hepatic stellate cells) are not infected with HCV, the data were not recorded. We also co-cultured Huh-7.5.1 infected with HCV and LX-2 cells and examined them using *in situ* PLA. However, the interaction between NS3 protease and TβRI was not observed on the surface of LX-2 cells. Furthermore, we performed co-immunoprecipitation assays using recombinant NS3 and the extracellular domain of TβRI and TβRII. As shown in Figure 3D, FLAG-tagged NS3 bound to TβRI and TβRII, whereas FLAG-tag alone failed to interact with TGF-β receptors (Fig. 3D and Supplementary Fig. S5).

Docking simulation using the Katchalski-Katzir algorithm predicted that NS3 interacts with TβRI at three sites, T22-S42, T76-P96, and G120-S139, in NS3 and F55-M70, I72-V85, and C86-Y99 in TβRI, respectively (Fig. 3E, Table 1, and Supplementary Fig. S6). The predicted binding site peptides, particularly the peptide derived from site 3, completely blocked the interaction between NS3 and